Report

Current Biology

Ancient *Yersinia pestis* and *Salmonella enterica* genomes from Bronze Age Crete

Highlights

- We provide genetic evidence of *Y. pestis* and *S. enterica* from Bronze Age Crete
- The *Y. pestis* genome is part of an extinct lineage of non-flea-adapted strains
- Ancient *S. enterica* genomes cluster with contemporary non-host-adapted strains
- The isolates coincide with societal changes ca. 2,000 BCE in Eastern Mediterranean

Authors

Gunnar U. Neumann, Eirini Skourtanioti, Marta Burri, ..., Maria A. Spyrou, Johannes Krause, Philipp W. Stockhammer

Correspondence

krause@eva.mpg.de (J.K.), philipp.stockhammer@lmu.de (P.W.S.)

In brief

Neumann et al. reconstruct ancient *Y. pestis* and *S. enterica* genomes from Crete around 2,000 BCE, a period of significant societal change in the region. Both strains are part of now-extinct lineages, but their existence suggests the importance of considering infectious diseases as a contributing factor to societal transformations.

Neumann et al., 2022, Current Biology *32*, 3641–3649
August 22, 2022
https://doi.org/10.1016/j.cub.2022.06.094

CellPress

Current Biology

CellPress
OPEN ACCESS

Report

Ancient *Yersinia pestis* and *Salmonella enterica* genomes from Bronze Age Crete

Gunnar U. Neumann,[1,2,3,11] Eirini Skourtanioti,[1,2,3] Marta Burri,[2,4] Elizabeth A. Nelson,[2,5] Megan Michel,[1,2,3,6] Alina N. Hiss,[1,2] Photini J.P. McGeorge,[7] Philip P. Betancourt,[8] Maria A. Spyrou,[1,2,9] Johannes Krause,[1,2,3,*] and Philipp W. Stockhammer[1,2,3,10,12,*]

[1]Department of Archaeogenetics, Max Planck Institute for Evolutionary Anthropology, Deutscher Platz 6, 04103 Leipzig, Germany
[2]Department of Archaeogenetics, Max Planck Institute for the Science of Human History, Kahlaische Str. 10, 07745 Jena, Germany
[3]Max Planck-Harvard Research Center for the Archaeoscience of the Ancient Mediterranean (MHAAM), Max Planck Institute for Evolutionary Anthropology, Deutscher Platz 6, 04103 Leipzig, Germany
[4]Swiss Ornithological Institute, Seerose 1, 6204 Sempach, Switzerland
[5]Department of Anthropology, University of Connecticut, 354 Mansfield Road, Storrs, CT 06269, USA
[6]Department of Human Evolutionary Biology, Harvard University, 10 Divinity Avenue, Cambridge, MA 02138, USA
[7]The British School at Athens, Souidias 52, Athens 106 76, Greece
[8]Department of Art History and Archaeology, Temple University, 2001 N. 13th St., Philadelphia, PA 19122, USA
[9]Institute for Archaeological Sciences, Eberhard Karls University of Tübingen, Hölderlinstr. 12, 72074 Tübingen, Germany
[10]Institute for Pre- and Protohistoric Archaeology and Archaeology of the Roman Provinces, Ludwig Maximilian University, Geschwister-Scholl-Platz 1, 80799 München, Germany
[11]Twitter: @gunnar_neumann
[12]Lead contact
*Correspondence: krause@eva.mpg.de (J.K.), philipp.stockhammer@lmu.de (P.W.S.)
https://doi.org/10.1016/j.cub.2022.06.094

SUMMARY

During the late 3rd millennium BCE, the Eastern Mediterranean and Near East witnessed societal changes in many regions, which are usually explained with a combination of social and climatic factors.[1–4] However, recent archaeogenetic research forces us to rethink models regarding the role of infectious diseases in past societal trajectories.[5] The plague bacterium *Yersinia pestis*, which was involved in some of the most destructive historical pandemics,[5–8] circulated across Eurasia at least from the onset of the 3rd millennium BCE,[9–13] but the challenging preservation of ancient DNA in warmer climates has restricted the identification of *Y. pestis* from this period to temperate climatic regions. As such, evidence from culturally prominent regions such as the Eastern Mediterranean is currently lacking. Here, we present genetic evidence for the presence of *Y. pestis* and *Salmonella enterica*, the causative agent of typhoid/enteric fever, from this period of transformation in Crete, detected at the cave site Hagios Charalambos. We reconstructed one *Y. pestis* genome that forms part of a now-extinct lineage of *Y. pestis* strains from the Late Neolithic and Bronze Age that were likely not yet adapted for transmission via fleas. Furthermore, we reconstructed two ancient *S. enterica* genomes from the Para C lineage, which cluster with contemporary strains that were likely not yet fully host adapted to humans. The occurrence of these two virulent pathogens at the end of the Early Minoan period in Crete emphasizes the necessity to re-introduce infectious diseases as an additional factor possibly contributing to the transformation of early complex societies in the Aegean and beyond.

RESULTS AND DISCUSSION

The Hagios Charalambos cave, situated on the Lasithi plateau of Crete, Greece (Figure 1), was used as a secondary burial site from the Late Neolithic (ca. 4th millennium Before Common Era [BCE]) to the Middle Minoan II period (18th century BCE)[14–16]. Secondary depositions of deceased individuals were a common practice during these periods on Crete,[17,18] but the Hagios Charalambos cave stands out as an ossuary that contains one of the largest corpora of human remains. In contrast to the low rates of ancient DNA (aDNA) recovery in the Eastern Mediterranean, Hagios Charalambos recently became known for its outstanding preservation of human aDNA,[19] probably due to its low and stable temperatures. Additionally, previous osteological analysis has identified a great number of pathologies in individuals deposited in this cave.[20,21] However, many diseases cannot be diagnosed by visual inspection of the remains alone because they do not leave any traces or lesions on bones, for example, in acute infections that do not last long enough or those occurring in different tissues of the body.[5] As teeth are highly vascularized during life-time, they can provide an excellent source for the detection of blood-borne pathogens in archaeogenetic studies.[22,23] In order to investigate which pathogens were present during the Bronze Age and their possible impact on early state societies in Crete, we analyzed 68 human teeth from the Hagios Charalambos cave. The selected specimens correspond

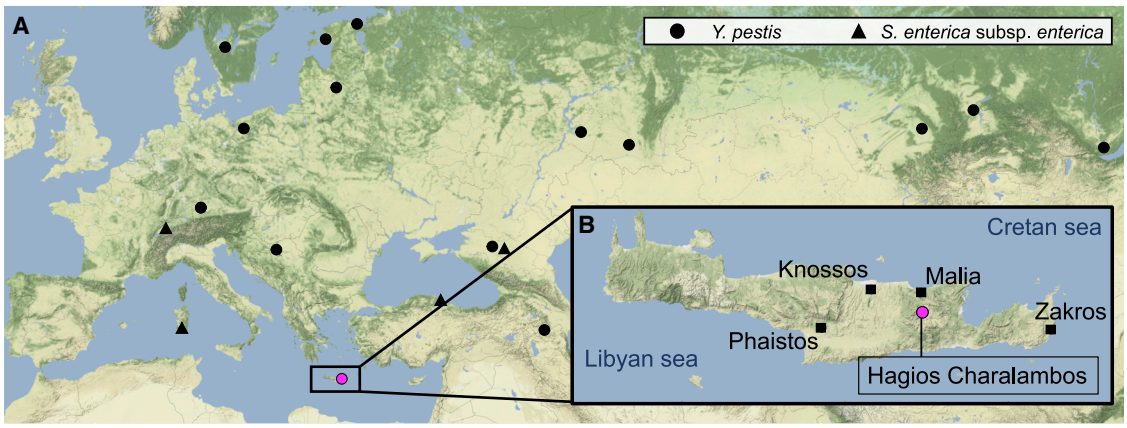

Figure 1. Location of archaeological sites with evidence of *Y. pestis* and *S. enterica* subsp. *enterica* from the LNBA

(A) Map of Eurasia indicating relevant LNBA sites with genetic evidence of *Y. pestis* (circles) and *S. enterica* subsp. *enterica* (triangles). Hagios Charalambos in pink, previously published sites in black.

(B) Map of Crete showing the location of Hagios Charalambos (pink) and important Bronze Age palatial sites (black).

to a minimum of 32 individuals (based on anthropological assessment), of which ten were radiocarbon-dated to between 2290 and 1909 calibrated BCE (calBCE, 2 sigma range; Table S1). The teeth were recovered from room 5 and had been found loose or in bone fragments on the floor. After extracting and shotgun sequencing the DNA from all 68 teeth, an estimation of human DNA preservation showed endogenous DNA percentages ranging from 0.1% to 34% (Table S2). A subsequent metagenomic analysis with the screening pipeline HOPS[24] for the investigation of pathogen presence in these specimens revealed traces of aDNA from a variety of common oral bacteria, such as the members of the so-called red complex (*Tannerella forsythia*, *Porphyromonas gingivalis*, and *Treponema denticula*) (Table S3), which passed the authentication criteria of (1) a declining edit distance distribution of reads that mapped to the reference genomes, (2) exhibiting a typical aDNA damage pattern in the form of C to T substitutions, and (3) an even distribution of mapped reads along the reference genomes. Intriguingly, we also detected the presence of ancient *Y. pestis* DNA in individuals HGC009 and HGC068, as well as *Salmonella enterica* DNA in individuals HGC004 and HGC040. All four individuals fulfilled the aforementioned criteria of the screening pipeline as possible candidates for whole-genome capture, with 14 non-duplicate reads in HGC009 assigned to the *Y. pestis* node, 30 reads in HGC068 assigned to the *Y. pseudotuberculosis* complex node, and 157 and 1,722 reads assigned to the *Salmonella enterica* subsp. *enterica* node for HGC004 and HGC040, respectively (Figure S1).

After whole-genome *S. enterica* enrichment of HGC004 and HGC040, read mapping against the Paratyphi C reference strain RKS4594 yielded a mean genomic coverage of 6.7- and 30.9-fold, respectively (Table 1). In a maximum likelihood (ML) phylogeny with other modern and ancient *S. enterica* genomes, both strains form a now-extinct clade together with SUA004 from Bronze Age Sardinia (2350–2060 calBCE) and the Late Neolithic OBP001 from Switzerland (3367–3118 calBCE)[25] (Figure 2A). This clade branches off basal to the Para C lineage, which includes the serovars Paratyphi C, Cholerasuis, Typhisuis, and Lomita. Similar to SUA004, both HGC genomes lack the *Salmonella* pathogenicity island SPI-7 (Figure S2), which is gained subsequently on the Para C lineage and is thus far identified among medieval and modern genomes of the Paratyphi C branch.[25,26] However, the *tcf*-operon, which is located on SPI-6 and lost in these medieval and modern Paratyphi C genomes, is still present in HGC004 and HGC040.

For *Y. pestis* analysis, libraries of HGC009 and HGC068 were enriched for *Y. pestis* DNA and reads mapped against the CO92 reference genome. For HGC009, this resulted in a mean coverage of 13.1-fold for the chromosome, 18.6-fold for the plasmid pMT1, 27.3-fold for pCD1, and 23.3-fold for pPCP1 (Table 1). Because the mean coverage of HGC068 was only 0.5-fold for the chromosome (pMT1: 0.6-fold, pCD1: 0.9-fold, pPCP1: 1.7-fold), with only 2.9% of the genome covered at least 3-fold, this sample was excluded from further analysis. An ML phylogeny showed HGC009 placement among previously published *Y. pestis* strains from the Late Neolithic and Bronze Age (LNBA),[10,11,13] within a basal branching *Y. pestis* lineage that has no modern descendants (Figure 2B). More specifically, HGC009 is positioned among the youngest identified LNBA isolates, being most closely related to the genome 6POST (2007–1882 calBCE) from Augsburg in Germany (SNP distance $d = 14$). In addition, consistent with all other ancient genomes of the LNBA lineage, HGC009 shows an absence of the *ymt* gene on the pMT1 plasmid (Figure S3) and exhibits the active forms of the genes *PDE-3*, *PDE-2*, *ureD, rscA*, and *flhD* (Figure S4). The latter are pseudogenized through insertions or nonsense mutations in all modern and historical *Y. pestis* genomes, but not in genomes of the LNBA lineage and the Middle Neolithic.[10,11] Inactivation of these genes in addition to the gain of *ymt* were important evolutionary steps for *Y. pestis* in its adaptation to the flea vector.[27–32] As such, the mode of transmission of the bacterium during its early evolution remains unclear.

It has been suggested that early *Y. pestis* dispersals across Eurasia followed human migration from the Eurasian steppe.[11] Such a hypothesis followed the observation that all LNBA

CellPress
OPEN ACCESS

Table 1. Metadata and summary statistics for pathogen reconstruction (2 sigma calBCE = 95% confidence interval calibrated Before Common Era based on AMS dating). See also Table S1

Individual	^{14}C-dating (2 σ calBCE)	Reference genome	Raw reads	Unique mapped reads	Mean coverage chromosome (X)	Coverage ≥ 3× [%]
HGC009	2036–1909	*Y. pestis* CO92 (chromosome)	76,670,971	1,259,2843	13.1	88.5
HGC068	N/A	*Y. pestis* CO92 (chromosome)	17,991,665	556,391.1	0.5	2.9
HGC004	2196–2034	*S. enterica* ParatyphiC RKS4594	32,405,434	523,608	6.7	80.6
HGC040	2280–2039	*S. enterica* ParatyphiC RKS4594	44,129,039	2,966,002	30.9	92.5

individuals from whom ancient *Y. pestis* genomes were isolated carried steppe-related ancestry in their genome and that the phylogeny of the LNBA *Y. pestis* genomes indicated the same directional spread. To investigate this observed correlation, we additionally enriched the HGC009 and HGC068 genomic libraries, as well as those of HGC004 and HGC040, for circa 1.24 million ancestry-informative SNPs on the human nuclear genome ("1240K SNP capture") of which 583,793 were successfully recovered in HGC009 and 285,259 in HGC040. Lower SNP yields were recovered for HGC068 (5,508 SNPs) and HGC004 (2,968 SNPs), and therefore, these specimens were not included in downstream analyses. Given this low number of SNPs, it cannot be excluded that samples HGC009 and HGC068 were teeth from the same individual, while the unique SNPs of the HGC004 and HGC040 *S. enterica* genomes indicate that these were two distinct strains, therefore infecting two different individuals. For HGC009 and HGC040, we performed a principal-component analysis (PCA) using modern West Eurasian populations as a scaffold onto which we projected HGC009, HGC040, and other relevant ancient populations. Our results revealed that both HGC009 and HGC040 cluster with other individuals from Hagios Charalambos and Moni Odigitria from Bronze Age Crete.[19] They are all shifted from the cluster of Greek Neolithic genomes in the direction of Chalcolithic-Bronze Age Anatolia (Figure 3A). With *qpAdm*,[33] we showed that similar to the other Bronze Age individuals from Crete,[19] HGC009 and HGC040 can be adequately modeled with additional ancestry from eastern sources, notably Chalcolithic Anatolia and the Caucasus (Figure 3B) or Chalcolithic Iran (Iran_C) (p values > 0.05). However, only models with Chalcolithic Anatolia fit when the target is the group of all the other individuals from Hagios Charalambos.[19] Models with sources representing the Bronze Age "steppe" ancestry (e.g., Samara-Caucasus Steppe), or LNBA Central Europeans who received gene flow from the former (e.g., C. Europe associated with the Corded Ware phenomenon), consistently failed at all times (p values for fit model to the data <<0.05). In contrast to the evidence from the rest of Europe, this indicates that if the disease reached Bronze Age Crete through contact with mobile peoples from outside Crete and non-related to Anatolia, they were small in number and left no trace in the Early

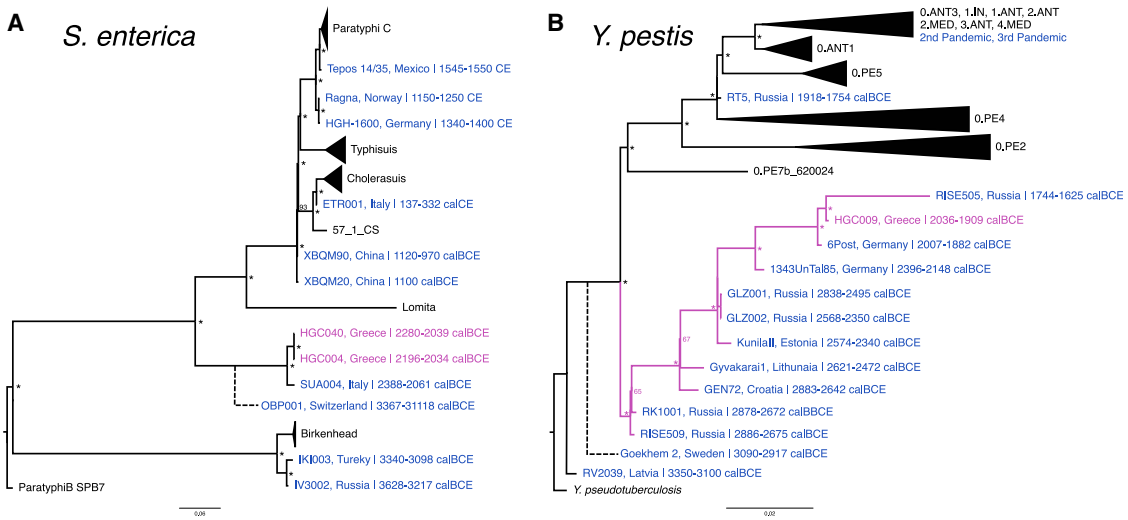

Figure 2. ML phylogenies of *S. enterica* and *Y. pestis*. Genomes from Hagios Charalambos in pink, previously published ancient genomes in blue, and modern genomes in black

Asterisks indicate bootstrap values of >95.

(A) *S. enterica* subsp. *enterica* ParaC lineage phylogeny based on 51,358 SNPs. OBP001 was added manually because of its low coverage, and the dashed line indicates its approximate position according to Key et al.[25]

(B) *Y. pestis* phylogenetic tree based on 5,317 SNPs with 98% partial deletion. The LNBA branch including HGC009 is colored in pink. Goekhem2 was added manually due to the low coverage of its genome, and the dashed line shows its approximate position according to Rascovan et al.[12]

See also Figures S1–S4

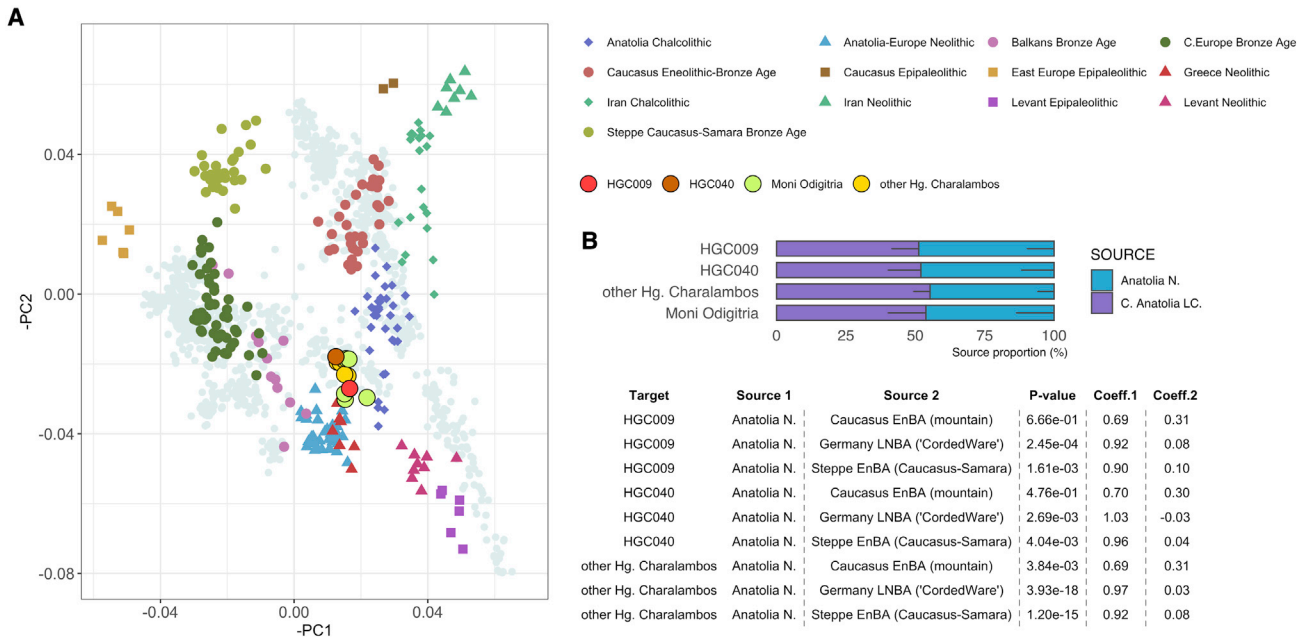

Target	Source 1	Source 2	P-value	Coeff.1	Coeff.2
HGC009	Anatolia N.	Caucasus EnBA (mountain)	6.66e-01	0.69	0.31
HGC009	Anatolia N.	Germany LNBA ('CordedWare')	2.45e-04	0.92	0.08
HGC009	Anatolia N.	Steppe EnBA (Caucasus-Samara)	1.61e-03	0.90	0.10
HGC040	Anatolia N.	Caucasus EnBA (mountain)	4.76e-01	0.70	0.30
HGC040	Anatolia N.	Germany LNBA ('CordedWare')	2.69e-03	1.03	-0.03
HGC040	Anatolia N.	Steppe EnBA (Caucasus-Samara)	4.04e-03	0.96	0.04
other Hg. Charalambos	Anatolia N.	Caucasus EnBA (mountain)	3.84e-03	0.69	0.31
other Hg. Charalambos	Anatolia N.	Germany LNBA ('CordedWare')	3.93e-18	0.97	0.03
other Hg. Charalambos	Anatolia N.	Steppe EnBA (Caucasus-Samara)	1.20e-15	0.92	0.08

Figure 3. Scatter plot of first two principal components and summary *qpAdm* models and estimated coefficients

(A) PCA was run on modern West Eurasian populations (Human Origins SNP panel; gray symbols), and the ancient individuals (colored symbols) were projected on top. The coordinates of previously published Minoan individuals from Hagios Charalambos and Moni Odigitria are also provided.

(B) Best fitting two-way model (p value $\geq$ 0.9) for HGC009 and other Bronze Age Cretan groups is presented as barplots with -1 SE. Model details for other tested possible proximal two-way models for Hagios Charalambos are provided in the table.

Bronze Age archaeogenetic record of the island. Whereas direct human-to-human contact based on the island's interconnectedness through mobility and trade is one possible way, the involvement of wild and/or domestic animals as hosts also needs to be considered, as plague is a zoonotic disease.

The genetic data suggest that the individuals investigated here were most probably inhabitants of Crete, living at the end of the 3rd millennium BCE (2290–1909 calBCE). This period is of special interest because it witnessed a series of major transformations across the Eastern Mediterranean, most notably the collapse of the Egyptian Old Kingdom and the Near Eastern Akkadian State.[1,2] The reasons for these developments have long been under debate, whereby climatic factors and especially severe droughts were emphasized as consequences of the so-called 4.2 ka BP climatic event.[2] In the Aegean, the late 3rd millennium (Early Helladic III) witnessed the decline of the complex interconnected societies that had emerged around 2700 BCE on the Greek mainland (Early Helladic II).[3,34] This drastic change was commonly explained by various reasons, such as environmental factors (e.g., erosion due to excessive land use), or climate and the migration or even invasion of people,[4,34,35] but only rarely were infectious diseases taken into consideration.[36] Additionally, the proposed events are not clearly visible across all potentially affected regions. On Crete, there is no apparent crisis at the end of the Early Minoan II period, and the transition between Early Minoan III and Middle Minoan IA periods (ca. 2300–2000/1900 BCE) is not clearly understood. These periods are nevertheless of particular importance because they directly preceded the emergence of the well-known Old Palaces during Middle Minoan IB at the very latest. Although some scholars have described continuity for this period,[37,38] others have argued for a phase of societal and population decline in large parts of Crete during Early Minoan III. They report the abandonment of a number of settlements and the subsequent formation of new ones, shortly before the building of the first palaces started in Middle Minoan IB around 1900 BCE.[39,40]

Both pathogens, *Y. pestis* and *S. enterica* subsp. *enterica*, which were identified in this study at the site of Hagios Charalambos from this time of transition, can cause severe epidemics in human populations. *Y. pestis* was responsible for at least three major pandemics in human history: the Justinianic plague, or first pandemic (540/41–750 CE), the Black Death/second pandemic (ca. 1346 until the 18th century CE), and the third pandemic (1855 until mid-20th century CE).[5] Archaeogenetic studies have shown that this pathogen was already present in a wide geographic range between central Europe and Siberia from the Middle Neolithic onward and especially during the Bronze Age.[9–13] However, genetic evidence for the presence of *Y. pestis* in the Eastern Mediterranean during this period has been lacking so far. The *S. enterica* genomes from Hagios Charalambos are part of the so-called Para C lineage, which comprises the three serovars Paratyphi C, Typhisuis, and Cholerasuis. At present, *S. enterica* Paratyphi C, together with Typhi, Paratyphi A and B, account for ca. 6 million cases of enteric fever in humans annually, with an estimated 54,000 deaths worldwide.[41] Ancient genomes from the Paratyphi C serovar were recently isolated from individuals of two medieval mass burials in the north German city of Lübeck, dating to the second half of the 14th century, suggesting an outbreak of paratyphoid fever.[42] It was also identified at a 16th century mass burial site in

Mexico city, which is associated with the devastating "cocoliztli" epidemic.[43]

The ancient pathogen genomes presented here belong to lineages of *Y. pestis* and *S. enterica* that lack any modern representatives. In addition, the *Y. pestis* genome is possibly not yet adapted to effective transmission via the flea vector and thus might have caused a different form of plague than the bubonic one, which is caused after the bacterium enters the lymphatic system from the location of the flea bite.Possible routes are the less efficient early phase transmission, which does not require blockage of the flea gut through biofilm formation,[44–47] airborne transmission (as in the pneumonic form of plague, which has been previously proposed),[48] or similarly to its closest relative, *Yersinia pseudotuberculosis*, via the fecal-oral route. As such, modern *Y. pestis* strains have the potential to also infect a variety of domesticated animals[49–51] and can be transmitted to humans through the consumption of contaminated meat[49,52–54] or the handling of the infected animals.[55] As for *S. enterica*, the serovars Paratyphi C, Typhisuis, and Cholerasuis, which account for the majority of strains in the Para C lineage, are restricted to humans and/or pigs as their hosts. Consistent with the fact that pseudogenization has been linked to host adaptation,[26,56,57] these strains show a higher number of pseudogenes than other non-host restricted *S. enterica* serovars.[25] However, the frequency of pseudogenes in ancient strains from this lineage, such as ETR001 and XBQM20/XBQM90, as well as SUA004, with which HGC004 and HGC040 form a distinct branch, is in the range of non-host adapted serovars, suggesting that these strains were rather host generalists.[25,58] In addition, these ancient genomes are lacking the *Salmonella* pathogenicity island SPI-7, which comprises a series of virulence genes including the Vi capsular polysaccharide operon.[59,60] It is associated with evasion of the immune system and typhoid fever and is present in only a few serovars, such as the human restricted serovars Typhi and Paratyphi C.

Therefore, the virulence and mode of transmission of these two pathogen strains from Hagios Charalambos remains uncertain, as does their potential to cause epidemic events. Moreover, their impact on the population and societies of Crete, especially during the transition from the Early Minoan III to Middle Minoan I, is difficult to infer from a restricted dataset derived from a single archaeological site, specifically in the case of Hagios Charalambos where all human remains were recovered from secondary burials. Future screening of more individuals from this region and period for the presence of pathogens will be essential for providing a more detailed picture of infectious disease impact in this region during the end of the 3rd millenium BCE.

Nevertheless, the occurrence of these two pathogens on the island of Crete is of significance. Both *Y. pestis* and *S. enterica* were previously shown to have had a wide distribution in Eurasia during the same period,[10,11,13,25,58] and given the existence of well-established trading networks in the Bronze Age Eastern Mediterranean,[61–63] our findings suggest that both pathogens may have also been circulating in neighboring areas from which they were introduced. Further, if both pathogens were present in remote areas such as the Lasithi plateau, they possibly also reached larger settlements in other parts of Crete. There, higher population densities could have facilitated the transmission to a great number of individuals.

While it is unlikely that *Y. pestis* or *S. enterica* were the sole culprits responsible for the societal changes observed in the Mediterranean at the end of the 3rd millennium BCE, we propose that, given the aDNA evidence presented here, infectious diseases should be considered as an additional contributing factor; possibly in an interplay with climate and migration, which has been previously suggested.[36] Incoming peoples with their livestock could have introduced both diseases to which the local population may have not been previously exposed. Moreover, the massive droughts described in association with the 4.2 ka BP climatic event could have resulted in a shortage of clean drinking water and an immunologically weakened population with higher susceptibility to infectious diseases.[36,64] As infections by some pathogens, such as *Y. pestis* and *S. enterica*, are not manifested osteologically, these diseases and their impacts have often been unnoticed in the archaeological record in the absence of other evidence (e.g., multiple burials). Therefore, archaeogenetic studies provide an important tool to identify pathogens that affected past populations and, as a result, reveal a more complete picture of their lives and health as well as the pathogens' evolution.

STAR★METHODS

Detailed methods are provided in the online version of this paper and include the following:

- KEY RESOURCES TABLE
- RESOURCE AVAILABILITY
  - Lead contact
  - Materials availability
  - Data and code availability
- EXPERIMENTAL MODEL AND SUBJECT DETAILS
  - Archaeological information
  - Permits
- METHOD DETAILS
  - Sampling, library preparation, and sequencing
  - In-solution capture
- QUANTIFICATION AND STATISTICAL ANALYSIS
  - Pathogen DNA screening
  - *Y. pestis* data processing and genotyping
  - SNP calling, SNP evaluation and phylogenetic analysis of *Y. pestis*
  - *Y. pestis* virulence factor analysis
  - Genetic analysis of *Salmonella enterica* data
  - Genetic analyses on human 1240K data

SUPPLEMENTAL INFORMATION

Supplemental information can be found online at https://doi.org/10.1016/j.cub.2022.06.094.

ACKNOWLEDGMENTS

We would like to thank the colleagues and laboratory staff at the Max Planck Institute for the Science of Human History in Jena and the Max Planck Institute for Evolutionary Anthropology in Leipzig: in particular, Angela Mötsch, Aida Andrades Valtueña, Alexander Herbig, James Fellow Yates, Antje Wissgott, Guido Brandt, Rita Radzeviciute, Raphaela Stahl, Rodrigo Barquera, Raffaela Bianco, Zandra Fagernäs, Florian Knolle, Anja Furtwängler, and Franziska Aron, as well as the whole pathogen and MHAAM group for fruitful discussions

and their help with analyses and laboratory work. This study was funded by the Max Planck Society and the Max Planck-Harvard Research Center for the Archaeoscience of the Ancient Mediterranean.

AUTHOR CONTRIBUTIONS

G.U.N., M.A.S., E.S., J.K., and P.W.S. designed the research. G.U.N., M.A.S., and E.S. performed the research. P.P.B. and P.J.P.M. provided samples. G.U.N., M.B., M.M., A.N.H., and E.A.N. performed the laboratory work. G.U.N. and E.S. analyzed the data. G.U.N., P.W.S., M.A.S., and E.S. wrote the paper with contribution by all co-authors.

DECLARATION OF INTERESTS

The authors declare no competing interests.

Received: January 28, 2022
Revised: April 25, 2022
Accepted: June 30, 2022
Published: July 25, 2022

REFERENCES

1. Bárta, M. (2019). Analyzing Collapse: the Rise and Fall of the Old Kingdom (American University in Cairo Press).
2. Weiss, H. (2017). 4.2 ka BP Megadrought and the Akkadian Collapse. Megadrought and Collapse: From Early Agriculture to Angkor Edition (Oxford University Press), pp. 93–160.
3. Wiersma, C., and Voutsaki, S. (2016). Social Change in Aegean Prehistory (Oxbow Books).
4. Wiener, M.H. (2013). "Minding the gap": gaps, destructions, and migrations in the Early Bronze Age Aegean. Causes and consequences. Am. J. Archaeol. *117*, 581–592.
5. Spyrou, M.A., Bos, K.I., Herbig, A., and Krause, J. (2019). Ancient pathogen genomics as an emerging tool for infectious disease research. Nat. Rev. Genet. *20*, 323–340.
6. Keller, M., Spyrou, M.A., Scheib, C.L., Neumann, G.U., Kröpelin, A., Haas-Gebhard, B., Päffgen, B., Haberstroh, J., Ribera i Lacomba, A., Raynaud, C., et al. (2019). Ancient Yersinia pestis genomes from across Western Europe reveal early diversification during the First Pandemic (541–750). Proc. Natl. Acad. Sci. *116*, 12363–12372.
7. Bos, K.I., Schuenemann, V.J., Golding, G.B., Burbano, H.A., Waglechner, N., Coombes, B.K., McPhee, J.B., DeWitte, S.N., Meyer, M., Schmedes, S., et al. (2011). A draft genome of Yersinia pestis from victims of the Black Death. Nature *478*, 506–510.
8. Feldman, M., Harbeck, M., Keller, M., Spyrou, M.A., Rott, A., Trautmann, B., Scholz, H.C., Päffgen, B., Peters, J., McCormick, M., et al. (2016). A high-coverage Yersinia pestis genome from a sixth-century Justinianic Plague victim. Mol. Biol. Evol. *33*, 2911–2923.
9. Susat, J., Lübke, H., Immel, A., Brinker, U., Macāne, A., Meadows, J., Steer, B., Tholey, A., Zagorska, I., Gerhards, G., et al. (2021). A 5,000-year-old hunter-gatherer already plagued by Yersinia pestis. Cell Rep. *35*, 109278.
10. Rasmussen, S., Allentoft, M.E., Nielsen, K., Orlando, L., Sikora, M., Sjögren, K.G., Pedersen, A.G., Schubert, M., Van Dam, A., Kapel, C.M., et al. (2015). Early divergent strains of Yersinia pestis in Eurasia 5,000 years ago. Cell *163*, 571–582.
11. Andrades Valtueña, A., Mittnik, A., Key, F.M., Haak, W., Allmäe, R., Belinskij, A., Daubaras, M., Feldman, M., Jankauskas, R., Janković, I., et al. (2017). The Stone Age plague and its persistence in Eurasia. Curr. Biol. *27*, 3683–3691.e8.
12. Rascovan, N., Sjögren, K.G., Kristiansen, K., Nielsen, R., Willerslev, E., Desnues, C., and Rasmussen, S. (2019). Emergence and spread of basal lineages of Yersinia pestis during the Neolithic decline. Cell *176*, 295–305.e10.
13. Yu, H., Spyrou, M.A., Karapetian, M., Shnaider, S., Radzevičiūtė, R., Nägele, K., Neumann, G.U., Penske, S., Zech, J., Lucas, M., et al. (2020). Paleolithic to Bronze Age Siberians reveal connections with first Americans and across Eurasia. Cell *181*, 1232–1245.e20.
14. Betancourt, P.P. (2014). Hagios Charalambos: A Minoan Burial Cave in Crete: I. Excavation and Portable Objects, Volume Prehistory Monograph 47 (INSTAP).
15. Davaras, C. (2015). The Elusive Site of the Primary Burials of the Hagios Charalambos Cave: a Speculative Scenario. In Hagios Charalambos. A Minoan Burial Cave in Crete II, The Pottery (Prehistory Monographs 51), P.P. Betancourt, C. Davaras, and E. Stravopodi, eds. (INSTAP Academic Press), pp. 119–128.
16. Langford-Verstegen, L.C. (2016). Hagios Charalambos: A Minoan Burial Cave in Crete: II. The Pottery, *Vol 51* (INSTAP Academic Press).
17. Girella, L., and Todaro, S. (2016). Secondary Burials and the Construction of Group Identities in Crete between the Second Half of the 4th and 2nd Millennia BC. In An Archaeology of Prehistoric Bodies and Embodied Identities in the Eastern Mediterranean (Oxbow Books), pp. 171–179.
18. Herrero, B.L. (2014). Mortuary Behavior and Social Trajectories in Pre- And Protopalatial Crete, *Vol 44* (INSTAP Academic Press).
19. Lazaridis, I., Mittnik, A., Patterson, N., Mallick, S., Rohland, N., Pfrengle, S., Furtwängler, A., Peltzer, A., Posth, C., Vasilakis, A., et al. (2017). Genetic origins of the Minoans and Mycenaeans. Nature *548*, 214–218.
20. McGeorge, P.J.P. (2011). Trauma, surgery and prehistoric events. Πεπραγμένα Γ' Διεθνούς Κρητολογικού Συνεδρίου, *Volume Τόμος* (Φιλολογικός Σύλλογος «Ο Χρυσόστομος»), pp. 347–361.
21. McGeorge, P.J.P. (2020). Palaeo-oncological findings from prehistoric Crete. In Πάλαιο-Ογκολογία Ιστορική Ανασκόπηση του Καρκίνου από την Αρχαιότητα μέχρι τον 21 Αιώνα, Πρακτικά του 2ου Διεθνούς Συμποσίου της Ευρωπαϊκής Εταιρείας Ιστορίας της Ογκολογίας (Academy of Athens), pp. 81–91.
22. Drancourt, M., Aboudharam, G., Signoli, M., Dutour, O., and Raoult, D. (1998). Detection of 400-year-old Yersinia pestis DNA in human dental pulp: an approach to the diagnosis of ancient septicemia. Proc. Natl. Acad. Sci. USA *95*, 12637–12640.
23. Schuenemann, V.J., Bos, K., DeWitte, S., Schmedes, S., Jamieson, J., Mittnik, A., Forrest, S., Coombes, B.K., Wood, J.W., and Earn, D.J. (2011). Targeted enrichment of ancient pathogens yielding the pPCP1 plasmid of Yersinia pestis from victims of the Black Death. Proc. Natl. Acad. Sci. USA *108*, E746–E752.
24. Hübler, R., Key, F.M., Warinner, C., Bos, K.I., Krause, J., and Herbig, A. (2019). HOPS: automated detection and authentication of pathogen DNA in archaeological remains. Genome Biol. *20*, 280.
25. Key, F.M., Posth, C., Esquivel-Gomez, L.R., Hübler, R., Spyrou, M.A., Neumann, G.U., Furtwängler, A., Sabin, S., Burri, M., Wissgott, A., et al. (2020). Emergence of human-adapted Salmonella enterica is linked to the Neolithization process. Nat. Ecol. Evol. *4*, 324–333.
26. Zhou, Z., Lundstrøm, I., Tran-Dien, A., Duchêne, S., Alikhan, N.-F., Sergeant, M.J., Langridge, G., Fotakis, A.K., Nair, S., and Stenøien, H.K. (2018). Pan-genome analysis of ancient and modern Salmonella enterica demonstrates genomic stability of the invasive para C lineage for millennia. Curr. Biol. *28*, 2420–2428.e10.
27. Hinnebusch, B.J., Jarrett, C.O., and Bland, D.M. (2021). Molecular and genetic mechanisms that mediate transmission of Yersinia pestis by fleas. Biomolecules *11*, 210.
28. Zhou, D., and Yang, R. (2009). Molecular Darwinian evolution of virulence in Yersinia pestis. Infect. Immun. *77*, 2242–2250.
29. Sun, Y.-C., Jarrett, C.O., Bosio, C.F., and Hinnebusch, B.J. (2014). Retracing the evolutionary path that led to flea-borne transmission of Yersinia pestis. Cell Host Microbe *15*, 578–586.
30. Chouikha, I., and Hinnebusch, B.J. (2014). Silencing urease: a key evolutionary step that facilitated the adaptation of Yersinia pestis to the flea-borne transmission route. Proc. Natl. Acad. Sci. USA *111*, 18709–18714.

31. Chain, P.S., Carniel, E., Larimer, F.W., Lamerdin, J., Stoutland, P.O., Regala, W.M., Georgescu, A.M., Vergez, L.M., Land, M.L., and Motin. (2004). Insights into the evolution of Yersinia pestis through whole-genome comparison with Yersinia pseudotuberculosis. Proc. Natl. Acad. Sci. USA *101*, 13826–13831.

32. Minnich, S.A., and Rohde, H.N. (2007). A rationale for repression and/or loss of motility by pathogenic Yersinia in the mammalian host. Adv. Exp. Med. Biol. *603*, 298–310.

33. Patterson, N., Moorjani, P., Luo, Y., Mallick, S., Rohland, N., Zhan, Y., Genschoreck, T., Webster, T., and Reich, D. (2012). Ancient admixture in human history. Genetics *192*, 1065–1093.

34. Weiberg, E., and Finné, M. (2013). Mind or matter? People-environment interactions and the demise of Early Helladic II society in the northeastern Peloponnese. Am. J. Archaeol. *117*, 1–31.

35. Maran, J. (1998). Kulturwandel auf dem griechischen Festland und den Kykladen im späten 3 Jahrtausend v. Chr (Habelt Bonn).

36. Arnott, R. (2004). Disease and the prehistory of the Aegean. In Health in Antiquity (Routledge), pp. 34–53.

37. Driessen, J., Schoep, I., and Tomkins, P. (2012). Back to the Beginning: Reassessing Social and Political Complexity on Crete during the Early and Middle Bronze Age (Oxboow Books).

38. Brogan, T.M. (2013). "Minding the Gap": reexamining the Early Cycladic III "Gap" from the Perspective of Crete. A Regional Approach to Relative Chronology, Networks, and Complexity in the Late Prepalatial period. Am. J. Archaeol. *117*, 555–567.

39. Watrous, L.V., and Schultz, M. (2012). Early Minoan III-middle Minoan IA periods: disruption and social reorganization. In Archaeological Survey of the Gournia Landscape: A Regional History of the Mirabello Bay, Crete, in Antiquity, L.V. Watrous, D. Haggis, K. Nowicki, N. Vogeikoff-Brogan, and M. Schultz, eds. (INSTAP Academic Press).

40. Watrous, L.V. (1994). Review of Aegean prehistory III: Crete from earliest prehistory through the protopalatial period. Am. J. Archaeol. *98*, 695–753.

41. WHO. (2018). Typhoid and Other Invasive Salmonellosis. Vaccine-Preventable Diseases (Surveillance Standards). https://cdn.who.int/media/docs/default-source/immunization/vpd_surveillance/vpd-surveillance-standards-publication/who-surveillancevaccinepreventable-21-typhoid-r2.pdf.

42. Haller, M., Callan, K., Susat, J., Flux, A.L., Immel, A., Franke, A., Herbig, A., Krause, J., Kupczok, A., and Fouquet, G. (2021). Mass burial genomics reveals outbreak of enteric paratyphoid fever in the Late Medieval trade city Lübeck. Iscience *24*, 102419.

43. Vågene, Å.J., Herbig, A., Campana, M.G., Robles García, N.M., Warinner, C., Sabin, S., Spyrou, M.A., Andrades Valtueña, A., Huson, D., Tuross, N., et al. (2018). Salmonella enterica genomes from victims of a major sixteenth-century epidemic in Mexico. Nat. Ecol. Evol. *2*, 520–528.

44. Eisen, R.J., Bearden, S.W., Wilder, A.P., Montenieri, J.A., Antolin, M.F., and Gage, K.L. (2006). Early-phase transmission of Yersinia pestis by unblocked fleas as a mechanism explaining rapidly spreading plague epizootics. Proc. Natl. Acad. Sci. USA *103*, 15380–15385.

45. Vetter, S.M., Eisen, R.J., Schotthoefer, A.M., Montenieri, J.A., Holmes, J.L., Bobrov, A.G., Bearden, S.W., Perry, R.D., and Gage, K.L. (2010). Biofilm formation is not required for early-phase transmission of Yersinia pestis. Microbiology *156*, 2216–2225.

46. Johnson, T.L., Hinnebusch, B.J., Boegler, K.A., Graham, C.B., MacMillan, K., Montenieri, J.A., Bearden, S.W., Gage, K.L., and Eisen, R.J. (2014). Yersinia murine toxin is not required for early-phase transmission of Yersinia pestis by Oropsylla montana (Siphonaptera: Ceratophyllidae) or Xenopsylla cheopis (Siphonaptera: Pulicidae). Microbiology *160*, 2517–2525.

47. Eisen, R.J., Dennis, D.T., and Gage, K.L. (2015). The role of early-phase transmission in the spread of Yersinia pestis. J. Med. Entomol. *52*, 1183–1192.

48. Zimbler, D.L., Schroeder, J.A., Eddy, J.L., and Lathem, W.W. (2015). Early emergence of Yersinia pestis as a severe respiratory pathogen. Nat. Commun. *6*, 7487.

49. Christie, A.B., Chen, T.H., and Elberg, S.S. (1980). Plague in camels and goats: their role in human epidemics. J. Infect. Dis. *141*, 724–726.

50. Dai, R., Wei, B., Xiong, H., Yang, X., Peng, Y., He, J., Jin, J., Wang, Y., Zha, X., Zhang, Z., et al. (2018). Human plague associated with Tibetan sheep originates in marmots. PLoS Negl. Trop. Dis. *12*, e0006635.

51. Nichols, M.C., Ettestad, P.J., Vinhatton, E.S., Melman, S.D., Onischuk, L., Pierce, E.A., and Aragon, A.S. (2014). Yersinia pestis infection in dogs: 62 cases (2003–2011). J. Am. Vet. Med. Assoc. *244*, 1176–1180.

52. Kehrmann, J., Popp, W., Delgermaa, B., Otgonbayar, D., Gantumur, T., Buer, J., and Tsogbadrakh, N. (2020). Two fatal cases of plague after consumption of raw marmot organs. Emerg. Microbes Infect. *9*, 1878–1880.

53. Bin Saeed, A.A.B., Al-Hamdan, N.A., and Fontaine, R.E. (2005). Plague from eating raw camel liver. Emerging Infect. Dis. *11*, 1456–1457.

54. Arbaji, A., Kharabsheh, S., Al-Azab, S., Al-Kayed, M., Amr, Z.S., Abu Baker, M., and Chu, M.C. (2005). A 12-case outbreak of pharyngeal plague following the consumption of camel meat, in north–eastern Jordan. Ann. Trop. Med. Parasitol. *99*, 789–793.

55. Wong, D., Wild, M.A., Walburger, M.A., Higgins, C.L., Callahan, M., Czarnecki, L.A., Lawaczeck, E.W., Levy, C.E., Patterson, J.G., and Sunenshine, R. (2009). Primary pneumonic plague contracted from a mountain lion carcass. Clin. Infect. Dis. *49*, e33–e38.

56. Liu, W.-Q., Feng, Y., Wang, Y., Zou, Q.-H., Chen, F., Guo, J.-T., Peng, Y.-H., Jin, Y., Li, Y.-G., and Hu, S.- (2009). Salmonella paratyphi C: genetic divergence from Salmonella choleraesuis and pathogenic convergence with Salmonella typhi. PloS One *4*, e4510.

57. Langridge, G.C., Fookes, M., Connor, T.R., Feltwell, T., Feasey, N., Parsons, B.N., Seth-Smith, H.M., Barquist, L., Stedman, A., and Humphrey, T. (2015). Patterns of genome evolution that have accompanied host adaptation in Salmonella. Proc. Natl. Acad. Sci. USA *112*, 863–868.

58. Wu, X., Ning, C., Key, F.M., Andrades Valtueña, A., Lankapalli, A.K., Gao, S., Yang, X., Zhang, F., Liu, L., and Nie, Z. (2021). A 3,000-year-old, basal S. enterica lineage from Bronze Age Xinjiang suggests spread along the Proto-Silk Road. PLoS Pathog. *17*, e1009886.

59. Wilson, R.P., Winter, S.E., Spees, A.M., Winter, M.G., Nishimori, J.H., Sanchez, J.F., Nuccio, S.-P., Crawford, R.W., Tükel, Ç., and Bäumler, A.J. (2011). The Vi capsular polysaccharide prevents complement receptor 3-mediated clearance of Salmonella enterica serotype Typhi. Infect. Immun. *79*, 830–837.

60. Seth-Smith, H.M. (2008). SPI-7: Salmonella's Vi-encoding pathogenicity island. J. Infect. Dev. Ctries. *2*, 267–271.

61. Cline, E.H. (1994). Sailing the Wine-Dark Sea: International Trade and the Late Bronze Age Aegean, Volume BAR Internationnal Series (Tempus Reparatum).

62. Feldman, M.H. (2006). Diplomacy by Design: Luxury Arts and an "International Style" in the Ancient Near East, 1400–1200 BCE (University of Chicago Press).

63. Vandkilde, H. (2016). Bronzization: the Bronze Age as pre-modern globalization. Praehistorische Z *91*, 103–123.

64. Stanke, C., Kerac, M., Prudhomme, C., Medlock, J., and Murray, V. (2013). Health effects of drought: a systematic review of the evidence. PLoS Curr. *5*, 1–40.

65. Huson, D.H., Albrecht, B., Bağcı, C., Bessarab, I., Górska, A., Jolic, D., and Williams, R.B.H. (2018). MEGAN-LR: new algorithms allow accurate binning and easy interactive exploration of metagenomic long reads and contigs. Biol. Direct *13*, 6.

66. Yates, J.A.F., Lamnidis, T.C., Borry, M., Andrades Valtueña, A., Fagernäs, Z., Clayton, S., Garcia, M.U., Neukamm, J., and Peltzer, A. (2021). Reproducible, portable, and efficient ancient genome reconstruction with nf-core/eager. PeerJ *9*, e10947.

67. Schubert, M., Lindgreen, S., and Orlando, L. (2016). AdapterRemoval v2: rapid adapter trimming, identification, and read merging. BMC Res. Notes *9*, 88.

68. Li, H., and Durbin, R. (2009). Fast and accurate short read alignment with Burrows–Wheeler transform. Bioinformatics *25*, 1754–1760.

69. DePristo, M.A., Banks, E., Poplin, R., Garimella, K.V., Maguire, J.R., Hartl, C., Philippakis, A.A., del Angel, G., Rivas, M.A., Hanna, M., et al. (2011). A framework for variation discovery and genotyping using next-generation DNA sequencing data. Nat. Genet. *43*, 491–498.

70. Jónsson, H., Ginolhac, A., Schubert, M., Johnson, P.L.F., and Orlando, L. (2013). Damage2. 0: fast approximate Bayesian estimates of ancient DNA damage parameters. Bioinformatics *29*, 1682–1684.

71. Bos, K.I., Harkins, K.M., Herbig, A., Coscolla, M., Weber, N., Comas, I., Forrest, S.A., Bryant, J.M., Harris, S.R., Schuenemann, V.J., et al. (2014). Pre-Columbian mycobacterial genomes reveal seals as a source of New World human tuberculosis. Nature *514*, 494–497.

72. Kozlov, A.M., Darriba, D., Flouri, T., Morel, B., and Stamatakis, A. (2019). RAxML-NG: a fast, scalable and user-friendly tool for maximum likelihood phylogenetic inference. Bioinformatics *35*, 4453–4455.

73. Kumar, S., Stecher, G., Li, M., Knyaz, C., and Tamura, K. (2018). MEGA X: molecular evolutionary genetics analysis across computing platforms. Mol. Biol. Evol. *35*, 1547–1549.

74. Quinlan, A.R., and Hall, I.M. (2010). BEDTools: a flexible suite of utilities for comparing genomic features. Bioinformatics *26*, 841–842.

75. Core Team, R. (2017). R: A Language and Environment for Statistical Computing (R Foundation for Statistical Computing).

76. RStudio. (2019). RStudio: integrated development for R. RStudio, Inc., Boston, MA. https://www.rstudio. com/products/rstudio.

77. Wickham, H. (2016). ggplot2: Elegant Graphics for Data Analysis (Springer-Verlag).

78. Robinson, J.T., Thorvaldsdóttir, H., Winckler, W., Guttman, M., Lander, E.S., Getz, G., and Mesirov, J.P. (2011). Integrative genomics viewer. Nat. Biotechnol. *29*, 24–26.

79. Peltzer, A., Jäger, G.n., Herbig, A., Seitz, A., Kniep, C., Krause, J., and Nieselt, K. (2016). EAGER: efficient ancient genome reconstruction. Genome Biol. *17*, 60.

80. Renaud, G., Slon, V., Duggan, A.T., and Kelso, J. (2015). Schmutzi: estimation of contamination and endogenous mitochondrial consensus calling for ancient DNA. Genome Biol. *16*, 224.

81. Korneliussen, T.S., Albrechtsen, A., and Nielsen, R. (2014). ANGSD: analysis of next generation sequencing data. BMC Bioinformatics *15*, 356.

82. Patterson, N., Price, A.L., and Reich, D. (2006). Population structure and eigenanalysis. PLOS Genet. *2*, e190.

83. Price, A.L., Patterson, N.J., Plenge, R.M., Weinblatt, M.E., Shadick, N.A., and Reich, D. (2006). Principal components analysis corrects for stratification in genome-wide association studies. Nat. Genet. *38*, 904–909.

84. Dabney, J., Knapp, M., Glocke, I., Gansauge, M.-T., Weihmann, A., Nickel, B., Valdiosera, C., García, N., Pääbo, S., Arsuaga, J.-L., et al. (2013). Complete mitochondrial genome sequence of a Middle Pleistocene cave bear reconstructed from ultrashort DNA fragments. Proc. Natl. Acad. Sci. USA *110*, 15758–15763.

85. Rohland, N., Harney, E., Mallick, S., Nordenfelt, S., and Reich, D. (2015). Partial uracil–DNA–glycosylase treatment for screening of ancient DNA. Philos. Trans. R. Soc. Lond. B Biol. Sci. *370*, 20130624.

86. Gansauge, M.-T., Aximu-Petri, A., Nagel, S., and Meyer, M. (2020). Manual and automated preparation of single-stranded DNA libraries for the sequencing of DNA from ancient biological remains and other sources of highly degraded DNA. Nat. Protoc. *15*, 2279–2300.

87. Rohland, N., Glocke, I., Aximu-Petri, A., and Meyer, M. (2018). Extraction of highly degraded DNA from ancient bones, teeth and sediments for high-throughput sequencing. Nat. Protoc. *13*, 2447–2461.

88. Fu, Q., Meyer, M., Gao, X., Stenzel, U., Burbano, H.A., Kelso, J., and Pääbo, S. (2013). DNA analysis of an early modern human from Tianyuan Cave, China. Proc. Natl. Acad. Sci. USA *110*, 2223–2227.

89. Fu, Q., Hajdinjak, M., Moldovan, O.T., Constantin, S., Mallick, S., Skoglund, P., Patterson, N., Rohland, N., Lazaridis, I., and Nickel, B. (2015). An early modern human from Romania with a recent Neanderthal ancestor. Nature *524*, 216–219.

90. Mathieson, I., Lazaridis, I., Rohland, N., Mallick, S., Patterson, N., Roodenberg, S.A., Harney, E., Stewardson, K., Fernandes, D., and Novak, M. (2015). Genome-wide patterns of selection in 230 ancient Eurasians. Nature *528*, 499–503.

91. Haak, W., Lazaridis, I., Patterson, N., Rohland, N., Mallick, S., Llamas, B., Brandt, G., Nordenfelt, S., Harney, E., and Stewardson, K. (2015). Massive migration from the steppe was a source for Indo-European languages in Europe. Nature *522*, 207–211.

92. Warinner, C., Herbig, A., Mann, A., Fellows Yates, J.A., Weiß, C.L., Burbano, H.A., Orlando, L., and Krause, J. (2017). A robust framework for microbial archaeology. Annu. Rev. Genomics Hum. Genet. *18*, 321–356.

93. Bos, K.I., Herbig, A., Sahl, J., Waglechner, N., Fourment, M., Forrest, S.A., Klunk, J., Schuenemann, V.J., Poinar, D., and Kuch, M. (2016). Eighteenth century Yersinia pestis genomes reveal the long-term persistence of an historical plague focus. eLife *5*, e12994.

94. Spyrou, M.A., Keller, M., Tukhbatova, R.I., Scheib, C.L., Nelson, E.A., Valtueña, A.A., Neumann, G.U., Walker, D., and Alterauge, A. Phylogeography of the second plague pandemic revealed through analysis of historical Yersinia pestis genomes. Nat. Commun. 10, 1.

95. Spyrou, M.A., Tukhbatova, R.I., Wang, C.-C., Valtueña, A.A., Lankapalli, A.K., Kondrashin, V.V., Tsybin, V.A., Khokhlov, A., Kühnert, D., and Herbig, A. (2018). Analysis of 3800-year-old Yersinia pestis genomes suggests Bronze Age origin for bubonic plague. Nat. Commun. *9*, 2234.

96. Cui, Y., Yu, C., Yan, Y., Li, D., Li, Y., Jombart, T., Weinert, L.A., Wang, Z., Guo, Z., Xu, L., et al. (2013). Historical variations in mutation rate in an epidemic pathogen, Yersinia pestis. Proc. Natl. Acad. Sci. USA *110*, 577–582.

97. Kislichkina, A.A., Bogun, A.G., Kadnikova, L.A., Maiskaya, N.V., Solomentsev, V.I., Sizova, A.A., Dentovskaya, S.V., Balakhonov, S.V., and Anisimov, A.P. (2018). Six whole-genome assemblies of Yersinia pestis subsp. Microtus bv. ulegeica (Phylogroup 0.PE5) Strains Isolated from Mongolian Natural Plague Foci. Genome Announc. *6*. e00536–e00518.

98. Kislichkina, A.A., Bogun, A.G., Kadnikova, L.A., Maiskaya, N.V., Solomentsev, V.I., Dentovskaya, S.V., Balakhonov, S.V., and Anisimov, A.P. (2018). Nine whole-genome assemblies of Yersinia pestis subsp. Microtus bv. Altaica Strains Isolated from the Altai Mountain Natural Plague Focus (No. 36) in Russia. Genome Announc. *6*. e01440–e01417.

99. Kislichkina, A.A., Bogun, A.G., Kadnikova, L.A., Maiskaya, N.V., Platonov, M.E., Anisimov, N.V., Galkina, E.V., Dentovskaya, S.V., and Anisimov, A.P. (2015). Nineteen whole-genome assemblies of Yersinia pestis subsp. Microtus, including representatives of biovars caucasica, talassica, Hissarica, altaica, xilingolensis, and ulegeica. Genome Announc. *3*. e01342–e01315.

100. Kutyrev, V.V., Eroshenko, G.A., Motin, V.L., Nosov, N.Y., Krasnov, J.M., Kukleva, L.M., Nikiforov, K.A., Al'khova, Z.V., Oglodin, E.G., and Guseva, N.P. (2018). Phylogeny and classification of Yersinia pestis through the lens of strains from the plague foci of Commonwealth of Independent States. Front. Microbiol. *9*, 1106.

101. Eroshenko, G.A., Nosov, N.Y., Krasnov, Y.M., Oglodin, Y.G., Kukleva, L.M., Guseva, N.P., Kuznetsov, A.A., Abdikarimov, S.T., Dzhaparova, A.K., and Kutyrev, V.V. (2017). Yersinia pestis strains of ancient phylogenetic branch 0. ANT are widely spread in the high-mountain plague foci of Kyrgyzstan. PLoS One *12*, e0187230.

102. Morelli, G., Song, Y., Mazzoni, C.J., Eppinger, M., Roumagnac, P., Wagner, D.M., Feldkamp, M., Kusecek, B., Vogler, A.J., Li, Y., et al.

(2010). Yersinia pestis genome sequencing identifies patterns of global phylogenetic diversity. Nat. Genet. *42*, 1140–1143.

103. Zhgenti, E., Johnson, S.L., Davenport, K.W., Chanturia, G., Daligault, H.E., Chain, P.S., and Nikolich, M.P. (2015). Genome assemblies for 11 Yersinia pestis strains isolated in the Caucasus region. Genome Announc. *3*. e01030–e01015.

104. Yoon, S.H., Park, Y.-K., and Kim, J.F. (2015). PAIDB v2. 0: exploration and analysis of pathogenicity and resistance islands. Nucleic Acids Res. *43*, D624–D630.

105. Allentoft, M.E., Sikora, M., Sjögren, K.-G., Rasmussen, S., Rasmussen, M., Stenderup, J., Damgaard, P.B., Schroeder, H., Ahlström, T., and Vinner, L. (2015). Population genomics of Bronze Age Eurasia. Nature *522*, 167–172.

106. Broushaki, F., Thomas, M.G., Link, V., López, S., van Dorp, L., Kirsanow, K., Hofmanová, Z., Diekmann, Y., Cassidy, L.M., and Díez-del-Molino, D. (2016). Early Neolithic genomes from the eastern Fertile Crescent. Science *353*, 499–503.

107. de Barros Damgaard, P., Martiniano, R., Kamm, J., Moreno-Mayar, J.V., Kroonen, G., Peyrot, M., Barjamovic, G., Rasmussen, S., Zacho, C., and Baimukhanov, N. (2018). The first horse herders and the impact of early Bronze Age steppe expansions into Asia. Science *360*, eaar7711.

108. Feldman, M., Fernández-Domínguez, E., Reynolds, L., Baird, D., Pearson, J., Hershkovitz, I., May, H., Goring-Morris, N., Benz, M., and Gresky, J. (2019). Late Pleistocene human genome suggests a local origin for the first farmers of central Anatolia. Nat. Commun. *10*, 1218.

109. Fu, Q., Posth, C., Hajdinjak, M., Petr, M., Mallick, S., Fernandes, D., Furtwängler, A., Haak, W., Meyer, M., and Mittnik, A. (2016). The genetic history of ice age Europe. Nature *534*, 200–205.

110. Gamba, C., Jones, E.R., Teasdale, M.D., McLaughlin, R.L., Gonzalez-Fortes, G., Mattiangeli, V., Domboróczki, L., Kővári, I., Pap, I., and Anders, A. (2014). Genome flux and stasis in a five millennium transect of European prehistory. Nat. Commun. *5*, 5257.

111. González-Fortes, G., Jones, E.R., Lightfoot, E., Bonsall, C., Lazar, C., Grandal-d'Anglade, A., Garralda, M.D., Drak, L., Siska, V., and Simalcsik, A. (2017). Paleogenomic evidence for multi-generational mixing between Neolithic farmers and Mesolithic hunter-gatherers in the lower Danube basin. Curr. Biol. *27*, 1801–1810.e10.

112. Haber, M., Doumet-Serhal, C., Scheib, C., Xue, Y., Danecek, P., Mezzavilla, M., Youhanna, S., Martiniano, R., Prado-Martinez, J., and Szpak, M. (2017). Continuity and admixture in the last five millennia of Levantine history from ancient Canaanite and present-day Lebanese genome sequences. Am. J. Hum. Genet. *101*, 274–282.

113. Harney, É., May, H., Shalem, D., Rohland, N., Mallick, S., Lazaridis, I., Sarig, R., Stewardson, K., Nordenfelt, S., and Patterson, N. (2018). Ancient DNA from Chalcolithic Israel reveals the role of population mixture in cultural transformation. Nat. Commun. *9*, 3336.

114. Hofmanová, Z., Kreutzer, S., Hellenthal, G., Sell, C., Diekmann, Y., Díez-del-Molino, D., van Dorp, L., López, S., Kousathanas, A., and Link, V. (2016). Early farmers from across Europe directly descended from Neolithic Aegeans. Proc. Natl. Acad. Sci. USA *113*, 6886–6891.

115. Jeong, C., Balanovsky, O., Lukianova, E., Kahbatkyzy, N., Flegontov, P., Zaporozhchenko, V., Immel, A., Wang, C.-C., Ixan, O., and Khussainova, E. (2019). The genetic history of admixture across inner Eurasia. Nat. Ecol. Evol. *3*, 966–976.

116. Jones, E.R., Gonzalez-Fortes, G., Connell, S., Siska, V., Eriksson, A., Martiniano, R., McLaughlin, R.L., Gallego Llorente, M.G., Cassidy, L.M., and Gamba, C. (2015). Upper Palaeolithic genomes reveal deep roots of modern Eurasians. Nat. Commun. *6*, 8912.

117. Lazaridis, I., Nadel, D., Rollefson, G., Merrett, D.C., Rohland, N., Mallick, S., Fernandes, D., Novak, M., Gamarra, B., and Sirak, K. (2016). Genomic insights into the origin of farming in the ancient Near East. Nature *536*, 419–424.

118. Lazaridis, I., Patterson, N., Mittnik, A., Renaud, G., Mallick, S., Kirsanow, K., Sudmant, P.H., Schraiber, J.G., Castellano, S., and Lipson, M. (2014). Ancient human genomes suggest three ancestral populations for present-day Europeans. Nature *513*, 409–413.

119. Lipson, M., Szécsényi-Nagy, A., Mallick, S., Pósa, A., Stégmár, B., Keerl, V., Rohland, N., Stewardson, K., Ferry, M., and Michel, M. (2017). Parallel palaeogenomic transects reveal complex genetic history of early European farmers. Nature *551*, 368–372.

120. Mallick, S., Li, H., Lipson, M., Mathieson, I., Gymrek, M., Racimo, F., Zhao, M., Chennagiri, N., Nordenfelt, S., and Tandon, A. (2016). The Simons genome diversity project: 300 genomes from 142 diverse populations. Nature *538*, 201–206.

121. Mathieson, I., Alpaslan-Roodenberg, S., Posth, C., Szécsényi-Nagy, A., Rohland, N., Mallick, S., Olalde, I., Broomandkhoshbacht, N., Candilio, F., and Cheronet, O. (2018). The genomic history of southeastern Europe. Nature *555*, 197–203.

122. Meyer, M., Kircher, M., Gansauge, M.-T., Li, H., Racimo, F., Mallick, S., Schraiber, J.G., Jay, F., Prüfer, K., and De Filippo, C. (2012). A high-coverage genome sequence from an archaic Denisovan individual. Science *338*, 222–226.

123. Mittnik, A., Wang, C.-C., Pfrengle, S., Daubaras, M., Zariņa, G., Hallgren, F., Allmäe, R., Khartanovich, V., Moiseyev, V., and Tõrv, M. (2018). The genetic prehistory of the Baltic Sea region. Nat. Commun. *9*, 442.

124. Narasimhan, V.M., Patterson, N., Moorjani, P., Rohland, N., Bernardos, R., Mallick, S., Lazaridis, I., Nakatsuka, N., Olalde, I., and Lipson, M. (2019). The formation of human populations in South and Central Asia. Science *365*, eaat7487.

125. Olalde, I., Brace, S., Allentoft, M.E., Armit, I., Kristiansen, K., Booth, T., Rohland, N., Mallick, S., Szécsényi-Nagy, A., and Mittnik, A. (2018). The Beaker phenomenon and the genomic transformation of northwest Europe. Nature *555*, 190–196.

126. Prüfer, K., de Filippo, C., Grote, S., Mafessoni, F., Korlević, P., Hajdinjak, M., Vernot, B., Skov, L., Hsieh, P., and Peyrégne, S. (2017). A high-coverage Neandertal genome from Vindija Cave in Croatia. Science *358*, 655–658.

127. Seguin-Orlando, A., Korneliussen, T.S., Sikora, M., Malaspinas, A.-S., Manica, A., Moltke, I., Albrechtsen, A., Ko, A., Margaryan, A., and Moiseyev, V. (2014). Genomic structure in Europeans dating back at least 36,200 years. Science *346*, 1113–1118.

128. Raghavan, M., Skoglund, P., Graf, K.E., Metspalu, M., Albrechtsen, A., Moltke, I., Rasmussen, S., Stafford, T.W., Jr., Orlando, L., and Metspalu, E. (2014). Upper Palaeolithic Siberian genome reveals dual ancestry of Native Americans. Nature *505*, 87–91.

129. Skoglund, P., Mallick, S., Bortolini, M.C., Chennagiri, N., Hünemeier, T., Petzl-Erler, M.L., Salzano, F.M., Patterson, N., and Reich, D. (2015). Genetic evidence for two founding populations of the Americas. Nature *525*, 104–108.

130. Skourtanioti, E., Erdal, Y.S., Frangipane, M., Restelli, F.B., Yener, K.A., Pinnock, F., Matthiae, P., Özbal, R., Schoop, U.-D., and Guliyev, F. (2020). Genomic history of Neolithic to Bronze Age Anatolia, Northern Levant, and Southern Caucasus. Cell *181*, 1158–1175.e28.

131. Vyas, D.N., Al-Meeri, A., and Mulligan, C.J. (2017). Testing support for the northern and southern dispersal routes out of Africa: an analysis of Levantine and southern Arabian populations. Am. J. Phys. Anthropol. *164*, 736–749.

132. Wang, C.-C., Reinhold, S., Kalmykov, A., Wissgott, A., Brandt, G., Jeong, C., Cheronet, O., Ferry, M., Harney, E., and Keating, D. (2019). Ancient human genome-wide data from a 3000-year interval in the Caucasus corresponds with eco-geographic regions. Nat. Commun. *10*, 590.

STAR★METHODS

KEY RESOURCES TABLE

REAGENT or RESOURCE	SOURCE	IDENTIFIER
Biological samples		
Human archaeological remains	This study	HGC001-HGC068; ENA: PRJEB52494
Chemicals, peptides, and recombinant proteins		
0.5 M EDTA, pH 8.0	Thermo Fisher Scientific (Life Technologies)	Cat#EP0052
Proteinase K	Sigma-Aldrich	Cat#P2308-100MG
Guanidine hydrochloride	Sigma-Aldrich	Cat#G3272-500g
Ethanol	Merck	Cat#1009832511
2-Propanol	Merck	Cat#1070222511
3M Sodium Acetate buffer pH 5.2	Sigma-Aldrich	Cat#S7899-500ML
TE buffer pH 8.0 low EDTA	Panreac AppliChem	Cat#A8569,0500
Tween 20	Sigma-Aldrich	Cat#P9416-50ML
Water HPLC Plus	Sigma-Aldrich	Cat#34877-2.5L-M
ATP	New England Biolabs	Cat#P0756S
BSA 20 mg/ml	New England Biolabs	Cat#B9000S
Bst 2.0 DNA Polymerase	New England Biolabs	Cat#M0537S
dNTP Mix 25 mM each	Thermo Scientific	Cat#R1121
T4 DNA Polymerase	New England Biolabs	Cat#M0203L
T4 Polynucleotide Kinase	New England Biolabs	Cat#M0201L
Buffer Tango 10x	Thermo Scientific	Cat#BY5
USER Enzyme	New England Biolabs	Cat#M5505L
5 M Sodium chloride (NaCl)	Sigma-Aldrich	Cat#S5150-1L
Denhardt's solution	Sigma-Aldrich	Cat#D9905-5Ml
Tris-HCl, pH 8.0	Thermo Fisher Scientific (Life Technologies)	Cat#15568025
Pfu Turbo Cx Hotstart DNA Polymerase	Agilent Technoloogies	Cat#600412
Herculase II Fusion DNA Polymerase	Agilent Technologies	Cat#600679
T4 RNA ligation Buffer	New England Biolabs	Cat#B0216L
10% Criterion™ TBE-Urea Polyacrylamide Gel, 18 well, 30 μl	BioRad	Cat#3450089
2x TBE-Urea Sample Buffer	BioRad	Cat#1610768
Oligo Length Standards 20/100 Ladder	IDT	Cat#51-05-15-02
UltraPure™ TBE Buffer, 10X	Thermo Fisher Scientific (Life Technologies)	Cat#15581044
20x SCC Buffer	Thermo Fisher Scientific (Life Technologies)	Cat#AM9770
Dynabeads MyOne Streptavidin C1	Thermo Fisher Scientific (Life Technologies)	Cat#65002
SYBR® Gold Nucleic Acid Gel Stain (10,000X Concentrate in DMSO)	Thermo Fisher Scientific (Life Technologies)	Cat#S33102
Polyethyleneglycol 8000 50%	Jena Bioscience	Cat#CSS-256
FastAP Thermosensitive Alkaline Phosphatase	Thermo Scientific	Cat#EF0652
T4 DNA-Ligase	Thermo Scientific	Cat#EL0013

(*Continued on next page*)

Continued

REAGENT or RESOURCE	SOURCE	IDENTIFIER
Klenow fragment	Thermo Scientific	Cat#EP0052
20% SDS Solution	Serva	Cat#39575.01
Silica Magnetic Beads	G-Bioscience	Cat#GENO786-915
D1000 ScreenTapes	Agilent Technologies	Cat#5067-5582
D1000 Reagents	Agilent Technologies	Cat#5067-5583
Sodiumhydroxide Pellets	Fisher Scientific	Cat#10306200
Sera-Mag Speed CM	GE Healthcare Lifescience	Cat#GE65152105050250
Dynabeads MyOne Streptavidin T1	Thermo Fisher Scientific (Life Technologies)	Cat#65601
GeneRuler Ultra Low Range DNA Ladder	Thermo Fisher Scientific (Life Technologies)	Cat#SM1211
10x GeneAmp PCR Gold Buffer and MgCl2	Thermo Fisher Scientific (Life Technologies)	Cat#4379874
Human Cot-1 DNA	Thermo Fisher Scientific (Life Technologies)	Cat#15279011
UltraPure™ Salmon Sperm DNA Solution	Thermo Fisher Scientific (Life Technologies)	Cat#15632011
PEG 8000 Powder, Molecular Biology Grade	Promega	Cat#V3011
Critical commercial assays		
High Pure Viral Nucleic Acid Large Volume Kit	Roche	Cat#5114403001
DyNAmo Flash SYBR Green qPCR Kit	Thermo Fisher Scientific	Cat#F415L
MinElute PCR Purification Kit	QIAGEN	Cat#28006
Quick Ligation Kit	New England Biolabs	Cat#M2200L
Oligo aCGH/Chip-on-Chip Hybridization Kit	Agilent Technologies	Cat#5188-5220
HiSeq 4000 SBS Kit (50/75 cycles)	Illumina	Cat#FC-410-1001/2
HiSeq® 3000/4000 PE Cluster Kit	Illumina	Cat#PE-410-1001
QIAquick Nucleotide Removal Kit	Quiagen	Cat#28304
Oligo aCGH/Chip-on-Chip Hybridization Kit	Agilent Technologies	Cat#5188-5220
Deposited data		
Raw and analyzed data (European nucleotide archive)	This study	ENA: PRJEB52494
Oligonucleotides		
IS5 (AATGATACGGCGACCACCGA)	Sigma-Aldrich	N/A
IS6 (CAAGCAGAAGACGGCATACGA)	Sigma-Aldrich	N/A
IS7 (ACACTCTTTCCCTACACGACGC)	Sigma-Aldrich	N/A
IS8 (GTGACTGGAGTTCAGACGTGTGC)	Sigma-Aldrich	N/A
BO4.P7.part1.R (GTGACTGGAGTTCAG ACGTGTGCTCTTCCGATCT[Phos])	Sigma-Aldrich	N/A
BO6.P7.part2.R (CAAGCAGAAGACGG CATACGAGAT[Phos])	Sigma-Aldrich	N/A
BO8.P5.part1.R (GTGTAGATCTCGGT GGTCGCCGTATCATT[Phos])	Sigma-Aldrich	N/A
BO10.P5.part2.R (AGATCGGAAGAGC GTCGTGTAGGGAAAGAGTGT[Phos])	Sigma-Aldrich	N/A
Software and algorithms		
HOPS v0.2	Hübler et al.[24]	https://github.com/rhuebler/HOPS
MALTv0.4.0	Vågene et al.[43]	https://github.com/husonlab/malt
MaltExtract v1.5	Hübler et al.[24]	https://github.com/rhuebler/HOPS

(*Continued on next page*)

Continued

REAGENT or RESOURCE	SOURCE	IDENTIFIER
MEGAN-LR v6.21.16	Huson et al.[65]	https://uni-tuebingen.de/fakultaeten/mathematisch-naturwissenschaftliche-fakultaet/fachbereiche/informatik/lehrstuehle/algorithms-in-bioinformatics/software/megan6/
nf-core/eager v2.2.1 / v2.3.5	Yates et al.[66]	https://github.com/nf-core/eager
AdapterRemoval v2	Schubert et al.[67]	https://github.com/MikkelSchubert/adapterremoval
Fastx_trimmer v0.0.14	http://hannonlab.cshl.edu/fastx_toolkit/license.html	http://hannonlab.cshl.edu/fastx_toolkit/license.html
Bwa v0.7.17	Li and Durbin[68]	http://bio-bwa.sourceforge.net/
GATK v3.5/v4.1.7	DePristo et al.[69]	https://gatk.broadinstitute.org/hc/en-us
Samtools v1.3	http://www.htslib.org/doc/1.1/samtools.html	http://www.htslib.org/doc/1.1/samtools.html
bbmap v38.86	https://sourceforge.net/projects/bbmap	https://sourceforge.net/projects/bbmap
mapDamage v2.0.9	Jónsson et al.[70]	https://github.com/ginolhac/mapDamage
MultiVCFAnalyzer v0.0.87	Bos et al.[71]	https://github.com/alexherbig/MultiVCFAnalyzer
SNPEvaluation	Keller et al.[6]	https://github.com/andreasKroepelin/SNP_Evaluation
raxml-ng v0.9.0	Kozlov et al.[72]	https://github.com/amkozlov/raxml-ng
FigTree v1.4.4	http://tree.bio.ed.ac.uk/software/figtree	http://tree.bio.ed.ac.uk/software/figtree
MEGAX v10.1.8	Kumar et al.[73]	https://www.megasoftware.net
bedtools v2.25.0	Quinlan and Hall[74]	https://bedtools.readthedocs.io/en/latest/
R v3.5.3	R Core Team[75]	https://www.r-project.org
R studio v1.1.423	RStudio[76]	https://www.rstudio.com
Ggplot 2 package	Wickham[77]	https://cran.r-project.org/web/packages/ggplot2/index.html
IGV v2.4.8	Robinson et al.[78]	https://software.broadinstitute.org/software/igv/
EAGER v1.92.59	Peltzer et al.[79]	https://eager.readthedocs.io/en/latest/
Dedup v0.12.2	Peltzer et al.[79]	https://github.com/apeltzer/DeDup
trimBam	https://genome.sph.umich.edu/wiki/BamUtil:_trimBam	https://genome.sph.umich.edu/wiki/BamUtil:_trimBam
Schmutzi	Renaud et al.[80]	https://github.com/grenaud/schmutzi
ANGSD v0.910	Korneliussen et al.[81]	http://www.popgen.dk/angsd/index.php/ANGSD
pileupCaller	https://github.com/stschiff/sequenceTools/tree/master/src/SequenceTools	https://github.com/stschiff/sequenceTools/tree/master/src/SequenceTools
EIGENSOFT package v7.2.1	Patterson et al.[82] and Price et al.[83]	https://github.com/DReichLab/EIG
qpAdm ADMIXTOOLS v5.1	Patterson et al.[33]	https://github.com/DReichLab/AdmixTools

RESOURCE AVAILABILITY

Lead contact

Further information and requests for resources and reagents should be directed to and will be fulfilled by the lead contact, Philipp W. Stockhammer (philipp.stockhammer@lmu.de)

Materials availability

This study did not generate unique reagents

Data and code availability

- Raw sequencing data have been deposited at the European Nucleotide Archive under the accession number PRJEB52494.
- This study did not generate any unique code.
- Any additional information required to reanalyze the data reported in this paper is available from the lead contact upon request.

EXPERIMENTAL MODEL AND SUBJECT DETAILS

Archaeological information

The Hagios Charalambos cave (latitude 35.1772505, longitude 25.4410963) is situated 835 m above sea level on the Lasithi Plain on Crete, Greece (Figure 1). The cave was discovered accidentally in 1976 when road building destroyed the roofs of two of the outer chambers brimming with human remains. A rescue excavation was directed by Costis Davaras in 1982–1983 and many important findings were moved to the Archaeological Museum of Heraklion, Crete. One room, though, was intentionally left intact for future studies with more advanced technology and resources, and the cave was sealed with iron bars and concrete to prevent looting. When looters did break into the cave during 2000, a new team of excavators was assembled under the direction of Philip Betancourt, Costis Davaras and Eleni Stavropodi, and the auspices of the American School of Classical Studies. The excavations lasted from 2002 to 2003 and were published in two volumes.[14,16]

The human remains recovered from all campaigns were exceptionally preserved owing to low and stable temperatures of the cave. The disarticulated condition of the bones indicates that the cavern was used as an ossuary. There was little actual soil deposit in the cave and post-excavation, it was determined that the secondary deposition was a unique event and that there was no meaningful stratigraphy. The pottery found alongside the commingled human remains provides a date range for the primary burials spanning the Late Neolithic II (ca. 4th millennium BCE) to the Middle Minoan IIB (18th century BCE). The primary burials must have been re-deposited in the cave without concern for their original contexts, but with careful transportation of original grave goods. Stones intrusive to the cave suggest that the primary interments might be from built tombs, but no traces of tombs have been found so far. However, the Psychro Cave, only 1 kilometer distant, could have been the original location of the primary burials, which needed to be removed to purify it when Psychro became the focus of cult worship in the Middle Minoan period, coinciding chronologically with the use of Hagios Charalambos for secondary burials.[15]

In the Neolithic and Early Minoan periods primary burials in caves were common, but the Hagios Charalambos cave stands out as an ossuary that represents one of the largest and best-preserved corpora of human remains from this early period. Currently, 32,000 bone fragments have been catalogued and their study has shown a low percentage of immature individuals. This poor representation could be partly due to the greater fragility of immature remains. Some sub-adult remains present repetitive injuries to articulations that suggest involvement of the very young in arduous day-to-day tasks. There is evidence for a range of pathologies: traumas, arthropathies, spondyloarthropathies, neoplasm[21] endocrine and genetic disorders. Furthermore, there is evidence for procedures to treat head traumas performed by surgeons who laid down the foundations for head surgery long before the Hippocratic treatises were written.[20]

The teeth for the ancient pathogen screening were all collected from Room 5, several centimeters below the surface of the deposit and were loose, commingled with other skeletal elements. Since no direct association with other bones or artefacts could be established, the teeth of ten individuals were radiocarbondated at the CEZ Archaeometry gGmbH, Mannheim, Germany, using a MICADAS-type AMS (Table S1). Of these, teeth which represent individuals HGC004, HG009 and HGC040 were ^{14}C-dated to 2196-2034 (MAMS-37429), 2036-1909 calBCE (MAMS-45081) and 2280-2039 (MAMS-49762), respectively, confirming the proposed range suggested by pottery fragments.

Permits

Necessary permits for sample export and analyses were obtained from Ephorate of Paleoanthropology – Speleology, Greece, under protocol number 2397.

METHOD DETAILS

Sampling, library preparation, and sequencing

All laboratory work was performed at the cleanroom facilities dedicated to the work with ancient DNA (aDNA) of the Max Planck Institute for the Science of Human History in Jena, Germany.

Teeth were irradiated with UV light for 15-30 min from two sides and cut with an electric saw at the cemento-enamel junction to separate the crown and roots. With a dentist drill, 30-50 mg of powder were drilled out from the inner pulp chamber and the root canals (https://doi.org/10.17504/protocols.io.bqebmtan), and for samples HGC001-HGC056 DNA was extracted with a protocol modified after Dabney et al.[84] (https://doi.org/10.17504/protocols.io.baksicwe). For sample HGC009 an additional extract was prepared. From all extracts of samples HGC001-HGC036, 25 μl were turned into double-indexed, double-stranded (ds) Illumina libraries with previous partial USER enzyme treatment based on Rohland et al.[85] (https://doi.org/10.17504/protocols.io.bmh6k39e, https://doi.org/10.17504/protocols.io.bvt8n6rw), which partially repairs the deamination from damaged ancient DNA molecules by maintaining the signal only at the terminal 3' and 5' positions. For HGC009 two ds libraries were prepared from each extract. From samples HGC037-HGC056 as well as HGC004 and HGC009 double-indexed single-stranded (ss) libraries (no USER treatment) were prepared from 30 μl DNA extracts using a protocol that included an automated liquid-handling system.[86] The same protocol including automated DNA extraction[86,87] was used for samples HGC057-HGC068 starting from bone powder directly without manual DNA extraction.

All libraries except ss libraries from HGC004 and HGC009 were initially sequenced on an Illumina HiSeq4000 with a single-end setting (1 x 76+8+8 cycles) on average to five million reads each, and were screened for the presence of endogenous host (human)

and pathogenic DNA (see below). After in-solution capture (see below) for *Y. pestis*, the two ss and two ds libraries of HGC009 were sequenced on an Illumina HiSeq4000, and two ds libraries on an Illumina NextSeq500 with paired-end settings (2 x 76+8+8 cycles, all at ten million reads, and the captured ss library of HGC068 was sequenced on an Illumina HiSeq4000 to ten million reads in single-end setting. The ds library of HGC004 enriched for S. enterica was sequenced to ten million reads with paired-end settings and the ss libraries of both HGC004 and HGC040 with single-end setting to ten million reads and 50 million reads, respectively, all on an Illumina HiSeq4000. Libraries from all four individuals enriched for c. 1.2 million SNP targets across the human genome[88–90] were also sequenced on an Illumina HiSeq4000 with single-end setting for c. 23-60 million reads.

In-solution capture

HGC009 and HGC068 fulfilled the screening criteria to be positive for *Y. pestis* and all libraries were in-solution captured for the whole genome of *Y. pestis* with a probe set designed as described before[11] based on the following sequences as templates: CO92 chromosome (NC_003143.1), CO92 plasmid pMT1 (NC_003134.1), CO92 plasmid pCD1 (NC_003131.1), Pestoides F chromosome (NC_009381.1), KIM10 chromosome (NC_004088.1), and *Y. pseudotuberculosis* IP 32953 chromosome (NC_006155.1). As possibly positive for *Salmonella enterica* DNA as identified by pathogen screening, HGC004 and HGC040 were in-solution captured for *S. enterica*. The probe set was generated from 67 chromosomal and 45 plasmid sequences/assemblies representing the modern *S. enterica* diversity.[43] Additionally, libraries from all four individuals were enriched for 1,237,207 ancestry-informative positions across the human genome (1240K).[88–91] All libraries were amplified to a DNA concentration of 200–400 ng/μl with IS5 and IS6 primers and then captured according to a previously published and well established protocol.[88–90] Capture was performed in 96-well plates in two rounds to enrich for pathogen DNA and one round for 1240K, except the library of HGC009 which was captured two rounds as well.

QUANTIFICATION AND STATISTICAL ANALYSIS

Pathogen DNA screening

All samples were screened for the presence of pathogen DNA using the screening pipeline HOPS v0.2.[24] Adapters from reads of shotgun sequencing were clipped with AdapterRemoval v2[67] within the nf-core/eager v2.2.1 pipeline[66] and reads were then used as input in the first step of HOPS. Reads were mapped with MALT v.0.4.0[43] to a RefSeq Genome database which includes all complete bacterial and viral genomes as of 2017 as well as additional eukaryotic pathogens plus the human reference sequence GRCHh38. Mapping was performed with BlastN mode and semi-global alignment type, using a minimum identity of 90 % (–minPercent_identity) and top percent value (–topPercent). Minimum support (–minSupport) was set to 1. In the second step of HOPS, MaltExtract v1.5, the results were filtered with a custom-made list of pathogens (https://github.com/rhuebler/HOPS/blob/external/Resources/default_list.txt) and authenticated based on edit distance distribution to the reference genome with and without considering aDNA damage, the read distribution along the reference as well as the aDNA damage pattern. Here, the edit distance distribution is expected to show a negative correlation in the number of reads with the number of mismatches to the reference for positive candidates, i.e. there should be more reads with no or one mismatch compared to reads with 3 or more mismatches. In addition, the MALT generated ram6-files of putatively positive samples were visually inspected in MEGAN-LR v6.21.16[65] to check the mismatches and an even distribution of the mapped reads. Only HGC009 and HGC068 were considered true positives for *Y. pestis* and processed further by preparing more sequencing libraries (for HGC009) and in-solution capture. Both HGC004 and HGC040 were considered as possible candidates for *S. enterica* and captured as well (Figure S1). Samples HGC008 and HGC059 equally passed all HOPS filter steps for S. enterica (Table S3), however, an atypical damage pattern and a high number of mismatches of the assigned reads to the reference, which are not due to aDNA damage, led to the conclusion that these are false positives, and therefore the samples were not captured. Additionally, we identified common oral bacteria, such as those of the so-called 'red complex' (*Tannerella forsythia*, *Porphyromonas gingivalis* and *Treponema denticula*) and *Streptococcus mutans*, which passed all HOPS authentication criteria (Table S3). Given the close identity of further detected pathogenic taxa, as for example *Clostridium botulinum*, to other nonpathogenic environmental species that are very common in soil,[92] their identification and authentication was not further pursued in the context of this study, as it would require targeted enrichment.

Y. pestis data processing and genotyping

All sequencing data from *Y. pestis*-captured ds and ss libraries were processed with the nf-core/eager v2.2.1 pipeline.[66] Adapters were clipped and overlapping paired-end reads merged with AdapterRemoval v2.[67] Reads from USER enzyme treated ds libraries were trimmed one base pair from both 5' and 3' ends to remove possible aDNA damage with fastx_trimmer v0.0.14 from the FASTX-Toolkit (http://hannonlab.cshl.edu/fastx_toolkit/license.html) and quality filtered using the -q 30 flag. With the Borrows wheeler aligner bwa v0.7.17[68] reads were mapped against the *Y. pestis* reference genome CO92 chromosome (NC_003143.1) and plasmids pCD1 (NC_003131.1), pMT1 (NC_003134.1) and pPCP1 (NC_003132.1). First, they were mapped with relaxed parameters with a seed length set to 16 (–bwaalnl 16) and mismatches to 0.01(–bwaalnn 0.01) using a quality filter of 37 (–bam_mapping_quality_threshold 37). Duplicates were removed with MarkDuplicates of GATK v4.1.7.0.[69]

Because contamination of the samples with closely related organisms can lead to falsely called SNPs in later analysis,[8] mapped reads from HGC009 were extracted from the bam-files with samtools v1.3 bam2fq (http://www.htslib.org/doc/1.1/samtools.html) and the resulting fastq-files used as input for the MEGAN Alignment Tool MALT v0.4.0.[43] The MALT run was performed in BlastN

mode and with the SemiGlobal alignment type. The top percent value and minimum support for a node were set to 1, and the maximum number of alignments to 100. No minimum percent identity was defined (-m BlastN -at SemiGlobal -top 1 -sup 1 -mq 100). The fastq files were run against a previously costum-built MALT database, which is based on the NCBI nucleotide (nt) database (October 2017, uploaded to Zenedo: https://doi.org/10.5281/zenodo.4382154) and had been indexed with MALT using the malt-build command. The resulting rma6-files were then loaded in MEGAN-LR v6.21.16[65] and summed up reads which mapped to the *Y. pseudotuberculosis* complex node were extracted. For further mapping, these fasta files were turned into fastq files by artificially adding a quality score of 35 with the reformat.sh script from bbmap v38.86 (https://sourceforge.net/projects/bbmap). The fastq-files with the extracted reads were then mapped again to the CO92 reference genome with strict parameters for the ds libraries (–bwaalnl 32 and –bwaalnn 0.1) and relaxed parameters for the ss libraries as described before. Bam-files of ds libraries were merged as well as libraries of ss libraries within the eager-pipeline. Possible aDNA damage in the bam-file of the merged ss libraries was rescaled with mapDamage v2.0.9.[70] The rescaled bam-file was subsequently combined with the merged bam-file from the ds libraries and genotyping was performed with the UnifiedGenotyper of the Genome Analysis Tool Kit GATK v3.5[69] with the 'EMIT_ALL_SITES' option.

SNP calling, SNP evaluation and phylogenetic analysis of *Y. pestis*

Variance calling was performed with MultiVCFAnalyzer v0.0.87[71] using the vcf-file from the merged libraries of HGC009 together with ten published ancient LNBA plague genomes[10,11,13] as well as 22 ancient[6,7,9,93,94,95] and 226 modern *Y. pestis* genomes.[96–103] *Y. pseudotuberculosis* IP32953 was added as an outgroup. Only positions which were covered at least three times with a minimum quality score of 30 were called. Positions were called as homozygous for one base if at least 90 % of the covering reads showed this base, otherwise it was set to "N". Annotated repetitive regions, rRNAs, tRNAs and tmRNAs as well as regions which had been previously reported as noncore[96,102] and can act problematic during mapping were excluded.

SNPs unique to HGC009 were evaluated with the snpEvaluation tool[6] and assumed to be false positive if they fulfilled at least one of the following conditions: 1) the coverage at this position exceeded the mean coverage of 13.1 x more than threefold, 2) there is one or more heterozygous positions within a 50 base pair (bp) window around the SNP which is not due to aDNA damage, 3) there is one or more uncovered positions within a 50 bp window around the SNP. In total, fifteen in such way detected false positive SNPs were subsequently excluded while running MultiVCFAnalyzer again with the same settings as before (positions of SNPs on the CO92 reference genome which were excluded: 47,939, 234,331, 362,683, 481,841, 481,875, 916,388, 1,011,354, 1,035,698, 1,306,826, 1,587,091, 2,122,841, 2,732,783, 2,897,244, 3,985,662, 4,621,067). From the resulting snpAlignment.fasta file, all SNPs that were covered by at least 98 % of the analysed genomes were extracted (98 % partial deletion) with an in-house python script.

A maximum likelihood (ML) phylogenetic tree was calculated from the generated 98 % partial deletion SNP-alignment with raxml-ng v0.9.0[72] using the –all function under the GTR+G substitution model. Bootstrap values were calculated with the Felsenstein method under the autoMRE option, i.e. bootstrapping was stopped when the test reached convergence (after 900 replicates here). The tree was finally visualized in FigTree v1.4.4 (http://tree.bio.ed.ac.uk/software/figtree) and rooted with *Y. pseudotuberculosis*. The genome from Goekhem[12] was excluded from this analysis because of its low coverage, but was added by hand afterwards and placed according to its publication due its important position in the phylogeny (Figure 2B).

The pairwise genetic distance between HGC009 and 6POST was calculated within MEGAX v10.1.8[73] using pairwise deletion for missing data.

Y. pestis virulence factor analysis

In order to analyse for the presence and absence of previously reported virulence factors of *Y. pestis*,[28] data from HGC009 (before MALT-processing) were mapped to the *Y. pestis* reference genome CO92 (chromosome and all three plasmids) as described above but without quality filtering (–bam_mapping_quality_threshold 0). The coverage of 115 chromosomal genes as well as 37 genes on the pCD1, 6 genes on the pMT1 and the *pla* gene on the pPCP1 plasmids was calculated using bedtools v2.25.0.[74] Visualisation was performed in R studio v1.1.423[75,76] using the ggplot2 package[77] (Figure S3).

Pseudogenization of the virulence associated genes PDE-2, PDE-3, *ureD, rscA* and *flhD* through mutation or single-nucleotide deletions/insertions was one of the key steps in *Y. pestis* evolution for flea-adapted transmission.[29,30] Reads mapping to these genes were inspected visually in IGV v2.4.8[78] after the malted reads were additionally mapped to *Y. pestis* KIM (NC_004088.1) and *Y. pseudotuberculosis* IP32953 (Figure S4). PDE-2 and PDE-3 are phosphodiesterases involved in biofilm degradation. PDE-2 is inactivated by a frameshift through the insertion of a T at position 1,434,044 in CO92. PDE-3 is pseudogenized by a C to T change in the promoter region and nonsense G to A substitutions at positions 3,944,166 and 3,944,543 in *Y. pseudotuberculosis* IP32953.[29,31] The expression of *ureD* is essential for urease activity which however is toxic for fleas which is why the inactivation is important for survival in the flea gut and which happened through insertion of a six-G stretch at position 2,997,296 in CO92. *RscA* codes for a component of the Rcs system and inhibits biofilm formation. Inactivation happens through a 30 bp internal duplication as was described in the *Y. pestis* strain KIM.[29] *FlhD* is involved in flagella biosynthesis and is pseudogenized through a T insertion at position 1,892,659 in CO92.[32] While these genes are still active in all LNBA *Y. pestis* strains, they are inactivated in the Bronze strains RT5 from the Baikal region in Russia.[95]

Genetic analysis of *Salmonella enterica* data

Sequencing data of samples HGC004 and HGC040 after *Salmonella* whole genome enriched were processed similar to HGC009 in the *Y. pestis* analysis. With the nf-core/eager pipeline,[66] reads were mapped to the *S. enterica* Paratyphi C str. RKS4594 reference

genome (NC_012125) using strict parameters for ds and relaxed parameters for ss libraries. Bam-files were merged for each sample and genotyped with the UnifiedGenotyper of the GATK tools kit v3.5.[69] Variance calling was performed with MultiVCFanalyzer v0.0.87[71] using the same parameters as for *Y. pestis*, with nine ancient[25,42,43,58] and eighteen modern *S. enterica* genomes of the ParaC lineage. The *S. enterica* Paratyphi B SPB7 was added with the outgroup-function. Repetitive, phage- and recombination-related regions were excluded.[43] A ML phylogenetic tree was constructed from the resulting SNP alignment which comprised all 51,358 SNPs with raxml-ng v0.9.0[72] using the—all function and a GTR-G substitution model. Bootstraps were calculated with 1,000 iterations. The ML tree was visualized in FigTree and rooted with the outgroup (Figure 2A).

Using MEGAX v10.1.8[73] the pairwise genetic distance between HGC004 and HGC040 was calculated with pairwise deletion for missing data.

To check for the presence and absence of *Salmonella* pathogenicity islands SPI-1 to SPI-5 and SPI-7 to SPI-10, reads were mapped against the *S. enterica* Typhi CT18 strain (NC_003198.1) with the nf-core/eager v2.3.5 pipeline[66] as described before for the *Y. pestis* virulence analysis. Coverage of the genomic regions were calculated with bedtools v2.29.2[74] within the pipeline (–run_bedtools_coverage). Coordinates of the different SPIs on the Typhi CT18 chromosome for the annotated input bed-file were taken from PAIDB.[104] The reference for SPI-6 was taken from PAIDB for mapping as described before, and coordinates for selected genes were taken from the annotation of the Para C lineage.[26] Coverage data were all SPIs were combined and visualised in R studio v1.1.423[75,76] using the ggplot2 package[77] (Figure S2).

Genetic analyses on human 1240K data

To assess human DNA preservation, shotgun sequencing data of all samples were mapped with the Borrows wheeler aligner bwa v0.7.17[68] against the human reference genome hs37d5 with—bwaalnn 0.01 and a quality filter of 25 (–bam_mapping_quality_threshold 25) within the nf-core/eager v2.3.5 pipeline.[66] Duplicates were removed with MarkDuplicates of GATK v3.5[69] (Table S2).

Sequencing data of samples enriched for human DNA were demultiplexed and processed through EAGER v1.92.59[79] for FastQC, clipping of Illumina adaptors with AdapterRemoval v2,[67] mapping against the hs37d5 human reference with the Borrows wheeler aligner bwa v0.7.12[68] and a quality filter of 30, and then removal of PCR duplicates with dedup v0.12.2.[79] Sequencing data from different runs were merged at the level of bam files, and dedup was run again. A version of bam masked on the two (HGC009) and ten (HGC040) terminal bp was created with trimBam (https://genome.sph.umich.edu/wiki/BamUtil:_trimBam) to remove damage. The sex of HGC009 and HGC040 was estimated by comparing the coverage on X and Y chromosomes (both numbers normalized with the autosomal coverage), and determined a male and female individual, respectively. Contamination was estimated both on the mitochondrium (original bam file) with Schmutzi,[80] and on the Y chromosome of HGC009 (masked bam file) with the tool from ANGSD v0.910.[81] Both methods agreed to a low average contamination of c. 1%. A pileup on the 1240K array positions was generated and genotypes were called with pileupCaller (https://github.com/stschiff/sequenceTools/tree/master/src/SequenceTools) and the option –randomHaploid which represents a genotype by randomly choosing one read at each site. The final genotype file of HGC009 included transitions that were retained from the masked bam file and transversions from the original. The genotype file of HGC040 was generated from the original bam file with the option from pileupCaller –singleStrandMode, which effectively removes residual damage from ss libraries. The two genotype files were then merged with publicly available datasets from ancient and modern individuals.[19,33,90,91,105–132] These included data produced with the 1240K capture array, shotgun-sequencing or whole-genome capture data that were subsequently pulled down to 1240K markers, and modern populations genotyped on the Illumina 'Human Origins' Affymetrix array. A subset of the latter (West Eurasian populations only) were used to perform a principal component analysis with the tool *smartpca* from the EIGENSOFT package v7.2.1,[82,83] and the ancient datasets were projected on the PCs using the option '*lsqproject'* (Figure 3A). We modeled admixture proportions using *qpAdm* from the package ADMIXTOOLS v5.1[33] (Figure 3B). A detailed explanation of the method is given in Haak et al.[91] For the setting of the right (reference) populations we used worldwide modern populations from the Simons Genome Diversity Project (SGDP) (Mbuti, Ami, Mixe, Onge) and ancient populations grouped as follows:

1. Western European hunter-gatherers (WEHG; n=14)[90,109,116,119,121]
2. Eastern European hunter-gatherers (EEHG; n=6: I0124, I0211, I0963, Popovo2, UzOO77)[90,123]
3. Caucasus hunter-gatherers (CHG; n=2: KK1, SATP)[116]
4. Ancestral North Eurasian (ANE; n=2: MA1 and Afontovo Gora2)[128]
5. Iran Neolithic from Ganj Darej (n=8)[117]
6. Israel Natufian (n=6)[117]

For the tested admixing sources, ancient individuals were grouped as follows:

1. Anatolia_N (Neolithic Anatolia; n=30), from Barcın, Menteşe and Boncuklu sites[90,108,]
2. C. Anatolia_LC (Late Chalcolithic Central Anatolian Çamlıbel Tarlası; n=9)[130]
3. Germany_LNBA (Corded Ware) (n=11)[91]
4. Mountain Caucasus_EnBA (Eneolithic and Bronze Age Caucasus from mountain range, n=32; I1634, I1632, I1631, I1635, I1633, I1658, I1656, I1409, I1407, RISE396.SG, RISE397.SG, RISE407.SG, RISE408.SG, RISE412.SG, RISE413.SG,

RISE416.SG, RISE423.SG, ARM001, ARM002, I1720, I2051, I2056, I6266, I6267, I6268, I6272, KDC001, MK5004, MK5008, OSS001, SA6002, VEK007)[105,107,117,132]

5. Caucasus-Samara Steppe_EnBA (Eneolithic and Bronze Age Eurasian Steppe from Samara to the steppe environment of Caucasus, n=28; I0370, I0441, I0444, I0439, I0357, I0429, I0438, I0443, I7489, BU2001, GW1001, I1723, KBD001, LYG001, MK3003, MK5009, PG2001, PG2002, PG2004, RK1001, RK1003, RK1007, RK4001, RK4002, SA6003, SA6010, VJ1001, ZO2002)[90,132]
6. Iran_C (Chalcolithic Iran, n=20), from Seh Gabi, Hajji Firuz and Tepe Hissar[117,124]